

Long and Short Guidance in Score identity Distillation for One-Step Text-to-Image Generation

Mingyuan Zhou

The University of Texas at Austin and Google
mingyuan.zhou@mcombs.utexas.edu

Zhendong Wang

The University of Texas at Austin
zhendong.wang@utexas.edu

Huangjie Zheng

The University of Texas at Austin
huangjie.zheng@utexas.edu

Hai Huang

Google
haih@google.com

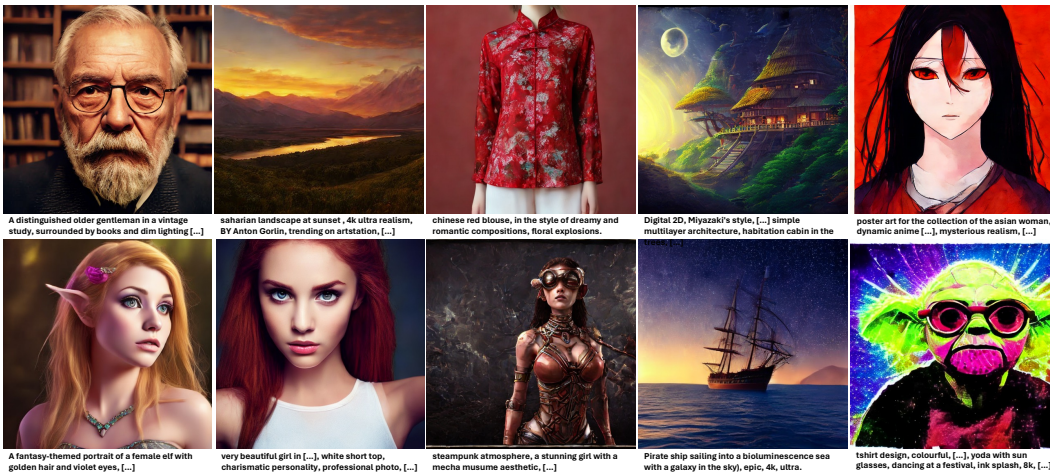


Figure 1: Example generation results of resolution 512x512 from the one-step generator distilled from Stable Diffusion 2.1-base using the proposed method: Score identity Distillation with Long-Short Guidance.

Abstract

Diffusion-based text-to-image generation models trained on extensive text-image pairs have shown the capacity to generate photorealistic images consistent with textual descriptions. However, a significant limitation of these models is their slow sample generation, which requires iterative refinement through the same network. In this paper, we enhance Score identity Distillation (SiD) by developing long and short classifier-free guidance (LSG) to efficiently distill pretrained Stable Diffusion models without using real training data. SiD aims to optimize a model-based explicit score matching loss, utilizing a score-identity-based approximation alongside the proposed LSG for practical computation. By training exclusively with fake images synthesized with its one-step generator, SiD equipped with LSG rapidly improves FID and CLIP scores, achieving state-of-the-art FID performance while maintaining a competitive CLIP score. Specifically, its data-free distillation of Stable Diffusion 1.5 achieves a record low FID of **8.15** on the COCO-2014 validation set, with a CLIP score of 0.304 at an LSG scale of 1.5, and a FID of 9.56 with a CLIP score of 0.313 at an LSG scale of 2. We will make our PyTorch implementation and distilled Stable Diffusion one-step generators available at <https://github.com/mingyuanzhou/SiD-LSG>.

1 Introduction

The pursuit of generating high-resolution, photorealistic images that matches the textual descriptions has consistently driven the machine learning community in developing powerful text-to-image generative models. Text-to-image diffusion models [Nichol et al., 2022, Ramesh et al., 2022, Saharia et al., 2022, Rombach et al., 2022, Podell et al., 2024] are currently leading the way in delivering unprecedentedly visual quality, diverse generation, and accurate text-image correspondences. They are renowned for their straightforward implementation and stability during optimization, and they receive substantial acclaim for the robust support from the open-source community [Rombach et al., 2022, Podell et al., 2024].

Despite these advantages, a significant limitation of diffusion models is their slow sampling process, which involves iterative refinement characterized by repeated forward passes through the generation network. Originally, this required a stochastic sampler with thousands of steps [Song and Ermon, 2019, Ho et al., 2020, Dhariwal and Nichol, 2021, Song et al., 2021a]. Recent advancements in deterministic samplers based on ordinary differential equations have significantly reduced the required number of sampling steps to just tens or hundreds [Song et al., 2021a, Liu et al., 2022a, Lu et al., 2022b, Karras et al., 2022].

To further reduce the number of steps below ten or make a single step diffusion-based generator, the focus has shifted toward distilling the iterative-refinement based multi-step text-to-image generative progress into a single or a few steps, using a wide variety of acceleration techniques [Zheng et al., 2023b, Meng et al., 2023, Liu et al., 2022b, Luo et al., 2023b, Nguyen and Tran, 2024, Sauer et al., 2023b, Xu et al., 2023, Yin et al., 2023]. However, they often result in clearly reduced ability to match the original data distribution, reflected as clearly worsening FIDs. All of them, with the exception of SwiftBrush [Nguyen and Tran, 2024], also require access to the original training data or the assistance of extra regression or adversarial losses.

It is commonly believed that student models used for distillation sacrifice performance for increased speed. However, recent findings from Score identity Distillation (SiD) [Zhou et al., 2024] present a notable discovery. The SiD-based single-step student model, although trained in a data-free manner, not only simplifies the multi-step generation process required by the teacher diffusion model, EDM by Karras et al. [2022], but also excels in performance. It surpasses the teacher model in terms of Fréchet inception distance (FID) [Heusel et al., 2017] on the CIFAR10-32x32, FFHQ-64x64, and AFHQ-v2 64x64 datasets. It only slightly underperforms in FID in comparison on ImageNet 64x64.

The success of SiD in distilling diffusion models in the pixel space has inspired us to apply it to open-source text-to-image latent diffusion models, specifically Stable Diffusion (SD) versions 1.5 and 2.1-base, aiming to significantly enhance their generation speed while maintaining performance. However, adapting SiD poses several notable challenges: first, SiD has primarily been applied to distill pre-trained EDM models, which utilize noise scheduling and preconditioning methods markedly different from the DDPM noise scheduling employed in SD; second, SiD-EDM does not incorporate classifier-free guidance (CFG) [Ho and Salimans, 2022], which is integral to SD; third, both the complexities and sizes of the data and model in EDM are much smaller than those in SD.

To address these challenges, we explore the integration of CFG into SiD-based diffusion distillation. We have developed strategies that either enhance CFG on the pretrained score network, reduce it on the fake score network, or apply a combination of both, known as long and short guidance (LSG). This method allows SiD to efficiently distill SD models into one-step generators without needing training data. Remarkably, without relying on additional regression or adversarial losses—key components of recent distillation methods—or real data, our approach sets new benchmarks by achieving the lowest zero-shot FID score of **8.15** on the COCO-2014 [Lin et al., 2014] validation set. This significantly outperforms all previous distillation methods while maintaining competitive CLIP scores.

The development of our SiD-LSG benefits tremendously from previous work on generative models, CFGs, and acceleration methods. We provide a detailed review of related work in Appendix B.

2 Empowering Score identity Distillation with long-short guidance

The effectiveness of SiD has been demonstrated in distilling both unconditional and label-conditional EDM-based diffusion models provided by Karras et al. [2022], which are pretrained on pixel spaces

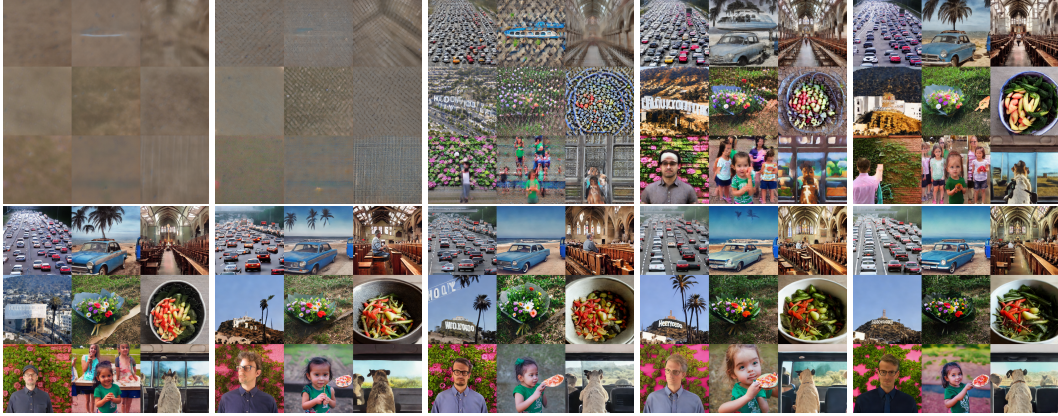


Figure 2: Rapid advancements in distilling Stable Diffusion 1.5 are showcased by the newly proposed SiD method, which employs long-short guidance (LSG). Key parameters include a batch size of 512, a learning rate of $1e-6$, and an LSG scale of 2. This data-free approach achieves a zero-shot FID of **9.56** on the COCO-2014 validation set, along with a competitive CLIP score of 0.313. By reducing the LSG scale to 1.5, the FID can be further lowered to a record **8.15** among diffusion distillation models, with a corresponding CLIP score of 0.304. The series of images, generated from the same set of random noises post-training the SiD generator with varying counts of synthesized images, illustrates progressions at 0, 0.02, 0.1, 0.2, 0.5, 1, 2, 3, 4, and 5 million images. These are equivalent to 0, 40, 200, 400, 1k, 2k, 4K, 6K, 8k, and 10k training iterations respectively, organized from the top left to the bottom right. The progression of FIDs and CLIPs is detailed in the orange solid curves in the left plot of Fig. 4. The corresponding COCO-2014 validation text prompts are listed in Appendix E.

up to a resolution of 64x64. In this paper, we expand the application of SiD to distill SD, the leading open-source platform for text-to-image diffusion models that operate on the latent space of an image encoder-decoder [Rombach et al., 2022]. Our focus is specifically on SD-v1-5 (SD1.5) and SD-v2-1-base (SD2.1-base), which are two versions extensively benchmarked for diffusion distillation.

The first challenge we tackle is adapting SiD, which was initially tested with EDM noise scheduling, to the classical DDPM scheduling employed by SD. A significant hurdle involves incorporating CFG [Ho and Salimans, 2022], which is essential for diffusion models to enhance their photorealism and text alignment, into the SiD loss functions. Addressing these challenges primarily requires modifying the derivation and loss functions of SiD. A third challenge arises because SD models are significantly larger and trained on data that is not only larger, but also more complex and of higher resolution. Overcoming this challenge requires addressing numerous technical details, such as establishing the minimum hardware requirements and computational precision. Additionally, it involves configuring the appropriate software settings to align with the constraints of the available computing platforms.

2.1 Semi-implicit distributions, score identities, and model-based score matching losses

We denote \mathbf{c} as the text representation of a pretrained text encoder, such as CLIP [Radford et al., 2021]. Our objective is to distill a student model $p_\theta(\mathbf{x}_g | \mathbf{c})$ from a pretrained text-to-image diffusion model, such as SD1.5, which can generate text-guided random samples in a single step as: $\mathbf{x}_g = G_\theta(\mathbf{z}, \mathbf{c})$, $\mathbf{z} \sim p(\mathbf{z})$, where G_θ is a neural network parameterized by θ that deterministically transforms noise $\mathbf{z} \sim p(\mathbf{z})$ into generated data \mathbf{x}_g under the guidance of text \mathbf{c} . The distribution of \mathbf{x}_g is often implicit [Mohamed and Lakshminarayanan, 2016, Tran et al., 2017, Yin and Zhou, 2018], lacking an analytic probability density function (PDF) but is straightforward to sample from. The marginals of the real and generated data under the forward diffusion process can be expressed as:

$$p_{\text{data}}(\mathbf{x}_t | \mathbf{c}) = \int q(\mathbf{x}_t | \mathbf{x}_0) p_{\text{data}}(\mathbf{x}_0 | \mathbf{c}) d\mathbf{x}_0, \quad p_\theta(\mathbf{x}_t | \mathbf{c}) = \int q(\mathbf{x}_t | \mathbf{x}_g) p_\theta(\mathbf{x}_g | \mathbf{c}) d\mathbf{x}_g.$$

This structure, characterized by explicit conditional layers but implicit marginals, exemplifies a semi-implicit distribution [Yin and Zhou, 2018, Yu et al., 2023]. This concept is employed by Zhou et al. [2024] to develop SiD, a method whose single-step data-free distillation capability has so far been demonstrated only on both unconditional and label-conditional diffusion models based on EDM.

We define the forward diffusion transition as $q(\mathbf{x}_t | \mathbf{x}_0) = \mathcal{N}(a_t \mathbf{x}_0, \sigma_t^2 \mathbf{I})$, and unlike in SiD, which adheres to EDM noise scheduling where $a_t = 1$, we allow a_t to vary within $[0, 1]$ to align with the DDPM scheduling used by SD during its training. This necessitates generalizing the equations used in SiD by permitting $a_t \neq 1$. We note that other diffusion types, such as categorical [Austin et al., 2021, Hooeboom et al., 2021, Gu et al., 2022, Hu et al., 2022], Poisson [Chen and Zhou, 2023], and beta diffusions [Zhou et al., 2023], also align with the semi-implicit framework and can potentially be adapted similarly.

Score identities. The scores $S(\mathbf{x}_t) := \nabla_{\mathbf{x}_t} \ln p_{\text{data}}(\mathbf{x}_t | \mathbf{c})$ and $\nabla_{\mathbf{x}_t} \ln p_{\theta}(\mathbf{x}_t | \mathbf{c})$ are generally unknown. However, the score of the forward conditional $q(\mathbf{x}_t | \mathbf{x}) \sim \mathcal{N}(\mathbf{x}, \sigma_t^2 \mathbf{I})$ is analytic:

$$\text{If } \mathbf{x}_t = a_t \mathbf{x} + \sigma_t \boldsymbol{\epsilon}_t, \boldsymbol{\epsilon}_t \sim \mathcal{N}(0, \mathbf{I}), \text{ then } \nabla_{\mathbf{x}_t} \ln q(\mathbf{x}_t | \mathbf{x}) = \sigma_t^{-2} (a_t \mathbf{x} - \mathbf{x}_t) = -\sigma_t^{-1} \boldsymbol{\epsilon}_t.$$

Exploiting the semi-implicit constructions, we follow SiD to present the following three identities:

$$\begin{aligned} \mathbb{E}[\mathbf{x}_0 | \mathbf{x}_t, \mathbf{c}] &= \int \mathbf{x}_0 q(\mathbf{x}_0 | \mathbf{x}_t, \mathbf{c}) d\mathbf{x}_0 = (\mathbf{x}_t + \sigma_t^2 \nabla_{\mathbf{x}_t} \ln p_{\text{data}}(\mathbf{x}_t | \mathbf{c}))/a_t, \\ \mathbb{E}[\mathbf{x}_g | \mathbf{x}_t, \mathbf{c}] &= \int \mathbf{x}_g q(\mathbf{x}_g | \mathbf{x}_t) d\mathbf{x}_g = (\mathbf{x}_t + \sigma_t^2 \nabla_{\mathbf{x}_t} \ln p_{\theta}(\mathbf{x}_t | \mathbf{c}))/a_t, \\ \mathbb{E}_{p_{\theta}(\mathbf{x}_t | \mathbf{c})} [u^T(\mathbf{x}_t) \nabla_{\mathbf{x}_t} \ln p_{\theta}(\mathbf{x}_t | \mathbf{c})] &= \mathbb{E}_{q(\mathbf{x}_t | \mathbf{x}_g) p_{\theta}(\mathbf{x}_g | \mathbf{c})} [u^T(\mathbf{x}_t) \nabla_{\mathbf{x}_t} \ln q(\mathbf{x}_t | \mathbf{x}_g, \mathbf{c})]. \end{aligned}$$

MESM loss. A pretrained text-to-image diffusion model, such as SD, provides a score network S_{ϕ} parameterized by ϕ that estimates the true data score as

$$-\sigma_t \nabla_{\mathbf{x}_t} \ln p_{\text{data}}(\mathbf{x}_t | \mathbf{c}) \approx -\sigma_t S_{\phi}(\mathbf{x}_t, \mathbf{c}) := \sigma_t^{-1} (\mathbf{x}_t - a_t f_{\phi}(\mathbf{x}_t, t, \mathbf{c})) = \boldsymbol{\epsilon}_{\phi}(\mathbf{x}_t, \mathbf{c}).$$

It adopts $f_{\phi}(\mathbf{x}_t, t, \mathbf{c})$ as the functional approximation of the conditional expectation of the real image \mathbf{x}_0 given noisy image \mathbf{x}_t and text \mathbf{c} , expressed as $\mathbb{E}[\mathbf{x}_0 | \mathbf{x}_t, \mathbf{c}]$, adopts $\boldsymbol{\epsilon}_{\phi}(\mathbf{x}_t, \mathbf{c})$ to predict the noise inside \mathbf{x}_t , and adopts $-\sigma_t^{-1} \boldsymbol{\epsilon}_{\phi}(\mathbf{x}_t, \mathbf{c})$ as the functional approximation of the true score $\nabla_{\mathbf{x}_t} \ln p_{\text{data}}(\mathbf{x}_t | \mathbf{c})$. Given time step $t \sim p(t)$ and text \mathbf{c} , we define the model-based explicit score-matching (MESM) distillation loss, which is a form of Fisher divergence [Lyu, 2009, Holmes and Walker, 2017, Yang et al., 2019, Yu and Zhang, 2023], as

$$\mathcal{L}_{\theta} = \mathbb{E}_{\mathbf{x}_t \sim p_{\theta}(\mathbf{x}_t)} [\|S_{\phi}(\mathbf{x}_t, \mathbf{c}) - \nabla_{\mathbf{x}_t} \ln p_{\theta}(\mathbf{x}_t | \mathbf{c})\|_2^2]. \quad (1)$$

Loss approximation for distillation. The MESM loss in (1) is in general intractable to compute as $\nabla_{\mathbf{x}_t} \ln p_{\theta}(\mathbf{x}_t | \mathbf{c})$ is unknown. To denoise the noisy fake data \mathbf{x}_t generated as

$$\mathbf{x}_t = a_t \mathbf{x}_g + \sigma_t \boldsymbol{\epsilon}_t, \boldsymbol{\epsilon}_t \sim \mathcal{N}(0, \mathbf{I}), \mathbf{x}_g = G_{\theta}(\mathbf{z}, \mathbf{c}), \mathbf{z} \sim p(\mathbf{z}), \quad (2)$$

there exists an optimal denoising network defined as $f_{\psi^*(\theta)}(\mathbf{x}_t, t, \mathbf{c}) = \mathbb{E}[\mathbf{x}_g | \mathbf{x}_t, \mathbf{c}] = (\mathbf{x}_t + \sigma_t^2 \nabla_{\mathbf{x}_t} \ln p_{\theta}(\mathbf{x}_t | \mathbf{c}))/a_t$. Given this optimal denoising network, the MESM loss in (1) would become

$$\mathcal{L}_{\theta} = \mathbb{E}_{\mathbf{x}_t \sim p_{\theta}(\mathbf{x}_t)} [\|a_t \sigma_t^{-2} (f_{\phi}(\mathbf{x}_t, t, \mathbf{c}) - f_{\psi^*(\theta)}(\mathbf{x}_t, t, \mathbf{c}))\|_2^2]. \quad (3)$$

As $\psi^*(\theta)$ is unknown in practice, approximation is needed. We follow SiD to introduce an approximate optimization algorithm that alternates between optimize ψ given θ using

$$\min_{\psi} \hat{\mathcal{L}}_{\psi}(\mathbf{x}_t, \mathbf{c}, t) = \frac{a_t^2}{\sigma_t^2} \|f_{\psi}(\mathbf{x}_t, t, \mathbf{c}) - \mathbf{x}_g\|_2^2 = \|\boldsymbol{\epsilon}_{\psi}(\mathbf{x}_t, t, \mathbf{c}) - \boldsymbol{\epsilon}_t\|_2^2, \quad (4)$$

and optimize θ given ψ using

$$\begin{aligned} \min_{\theta} \tilde{L}_{\theta}(\mathbf{x}_t, t, \phi, \psi) &= \omega(t) \frac{a_t^2}{\sigma_t^2} (f_{\phi}(\mathbf{x}_t, t, \mathbf{c}) - f_{\psi}(\mathbf{x}_t, t, \mathbf{c}))^T (f_{\psi}(\mathbf{x}_t, t, \mathbf{c}) - \mathbf{x}_g), \\ &= \omega(t) \frac{1}{\sigma_t^2} (\boldsymbol{\epsilon}_{\psi}(\mathbf{x}_t, t, \mathbf{c}) - \boldsymbol{\epsilon}_{\phi}(\mathbf{x}_t, t, \mathbf{c}))^T (\boldsymbol{\epsilon}_t - \boldsymbol{\epsilon}_{\psi}(\mathbf{x}_t, t, \mathbf{c})), \end{aligned} \quad (5)$$

where \mathbf{x}_t is generated as in (2) and $\omega(t)$ are weighted coefficients that will be specified. Note that (5) simplifies the corresponding one in SiD by fixing $\alpha = 1$, a parameter that can be tuned in SiD to enhance performance but fixed at one in this paper. We have strategically set $\alpha = 1$ to focus more on analyzing the injection of CFGs into SiD, leaving the tuning of this parameter for future work.

Algorithm 1 SiD-LSG: Score identity Distillation with Long-Short classifier-free Guidance

Input: Pretrained score network f_ϕ , generator G_θ , fake score network f_ψ , $t_{\text{init}} = 625$, $t_{\text{min}} = 20$, $t_{\text{max}} = 979$, guidance scales $\kappa_1 = \kappa_2 = \kappa_3 = \kappa_4 = 2$

Initialization $\theta \leftarrow \phi$, $\psi \leftarrow \phi$

repeat

Sample $\mathbf{z} \sim \mathcal{N}(0, \mathbf{I})$ and \mathbf{c} , and let $\mathbf{x}_g = G_\theta(\mathbf{z}, \mathbf{c}) = f_\theta(\sigma_{t_{\text{init}}}\mathbf{z}, t_{\text{init}}, \mathbf{c})$; Sample $t \in \{t_{\text{min}}, \dots, t_{\text{max}}\}$ and $\boldsymbol{\epsilon}_t \sim \mathcal{N}(0, \mathbf{I})$, and let $\mathbf{x}_t = a_t\mathbf{x}_g + \sigma_t\boldsymbol{\epsilon}_t$

Update ψ with $\psi = \psi - \eta\nabla_\psi \hat{\mathcal{L}}_\psi$, where

$$\hat{\mathcal{L}}_\psi = \frac{a_t^2}{\sigma_t^2} \|f_{\psi, \kappa_1}(\mathbf{x}_t, t, \mathbf{c}) - \mathbf{x}_g\|_2^2 = \|\boldsymbol{\epsilon}_{\psi, \kappa_1}(\mathbf{x}_t, t, \mathbf{c}) - \boldsymbol{\epsilon}_t\|_2^2$$

Sample $\mathbf{z} \sim \mathcal{N}(0, \mathbf{I})$ and let $\mathbf{x}_g = G_\theta(\sigma_{\text{init}}\mathbf{z})$; Sample $t \in \{t_{\text{min}}, t_{\text{min}} + 1, \dots, t_{\text{max}}\}$, compute ω_t with (9), and let $\mathbf{x}_t = \mathbf{x}_g + \sigma_t\boldsymbol{\epsilon}_t$

Update G_θ with $\theta = \theta - \eta\nabla_\theta \tilde{\mathcal{L}}_\theta$, where

$$\begin{aligned} \tilde{\mathcal{L}}_\theta &= \frac{\omega(t)a_t^2}{\sigma_t^4} (f_{\phi, \kappa_4}(\mathbf{x}_t, t, \mathbf{c}) - f_{\psi, \kappa_2}(\mathbf{x}_t, t, \mathbf{c}))^T (f_{\psi, \kappa_3}(\mathbf{x}_t, t, \mathbf{c}) - \mathbf{x}_g) \\ &= \frac{\omega(t)}{\sigma_t^2} (\boldsymbol{\epsilon}_{\psi, \kappa_4}(\mathbf{x}_t, t, \mathbf{c}) - \boldsymbol{\epsilon}_{\phi, \kappa_2}(\mathbf{x}_t, t, \mathbf{c}))^T (\boldsymbol{\epsilon}_t - \boldsymbol{\epsilon}_{\psi, \kappa_3}(\mathbf{x}_t, t, \mathbf{c})) \end{aligned}$$

until processing 10M fake images or the training budget is exhausted

Output: G_θ

2.2 SiD with classifier-free guidance

An essential practice for enhancing photorealism and alignment with text instructions in text-to-image diffusion models involves incorporating CFG into reverse diffusion. This principle also applies to distillation methods for these models, where CFG must be integrated into the appropriate terms of their distillation loss functions. Therefore, a key distinction in the distillation of SD, compared to previous unconditional and label-conditional diffusion models, lies in the need to introduce CFG.

SiD presents a unique opportunity to apply CFG to enhance its text-to-image generation performance. First, we note CFG enhances text guidance by modifying the distribution of \mathbf{x}_t given text \mathbf{c} as

$$p(\mathbf{x}_t | \mathbf{c}, \kappa) \propto p(\mathbf{c} | \mathbf{x}_t)^\kappa p(\mathbf{x}_t) \propto \left(\frac{p(\mathbf{x}_t | \mathbf{c})}{p(\mathbf{x}_t)} \right)^\kappa p(\mathbf{x}_t),$$

which means $\nabla_{\mathbf{x}_t} \ln p(\mathbf{x}_t | \mathbf{c}, \kappa) = \nabla_{\mathbf{x}_t} \ln p(\mathbf{x}_t) + \kappa[\nabla_{\mathbf{x}_t} \ln p(\mathbf{x}_t | \mathbf{c}) - \nabla_{\mathbf{x}_t} \ln p(\mathbf{x}_t)]$. Second, the score network, when reaching its optimal, is related to the true score as $f(\mathbf{x}_t, t, \mathbf{c}) = a_t^{-1}(\mathbf{x}_t + \sigma_t^2 \nabla_{\mathbf{x}_t} \ln p(\mathbf{x}_t | \mathbf{c})) = a_t^{-1}(\mathbf{x}_t - \sigma_t \boldsymbol{\epsilon}(\mathbf{x}_t, t, \mathbf{c}))$. Therefore, with “ \cdot ” representing ϕ or ψ , we can express the score network $f_\cdot(\mathbf{x}_t, t, \mathbf{c})$ under CFG with scale κ as

$$f_{\cdot, \kappa}(\mathbf{x}_t, t, \mathbf{c}) = f_\cdot(\mathbf{x}_t, t) + \kappa[f_\cdot(\mathbf{x}_t, t, \mathbf{c}) - f_\cdot(\mathbf{x}_t, t)]. \quad (6)$$

Similarly, for noise prediction network, we have $\boldsymbol{\epsilon}_{\cdot, \kappa}(\mathbf{x}_t, t, \mathbf{c}) = \boldsymbol{\epsilon}_\cdot(\mathbf{x}_t, t) + \kappa[\boldsymbol{\epsilon}_\cdot(\mathbf{x}_t, t, \mathbf{c}) - \boldsymbol{\epsilon}_\cdot(\mathbf{x}_t, t)]$. With CFG, the score and noise prediction networks are related in the same way, which means that $\boldsymbol{\epsilon}_{\cdot, \kappa}(\mathbf{x}_t, t, \mathbf{c}) = \sigma_t^{-1}(\mathbf{x}_t - a_t f_{\cdot, \kappa}(\mathbf{x}_t, t, \mathbf{c}))$ and $f_{\cdot, \kappa}(\mathbf{x}_t, t, \mathbf{c}) = a_t^{-1}(\mathbf{x}_t - \sigma_t \boldsymbol{\epsilon}_{\cdot, \kappa}(\mathbf{x}_t, t, \mathbf{c}))$.

Inspecting the two losses in (4) and (5) suggests four potential places to inject CFG. More specifically, with $\kappa_1, \kappa_2, \kappa_3, \kappa_4 \in \mathbb{R}_+$, where $\mathbb{R}_+ = \{x : x \geq 0\}$, we modify the losses with CFGs as

$$\hat{\mathcal{L}}_\psi(\mathbf{x}_t, \mathbf{c}, t) = \frac{a_t^2}{\sigma_t^2} \|f_{\psi, \kappa_1}(\mathbf{x}_t, t, \mathbf{c}) - \mathbf{x}_g\|_2^2 = \|\boldsymbol{\epsilon}_{\psi, \kappa_1}(\mathbf{x}_t, t, \mathbf{c}) - \boldsymbol{\epsilon}_t\|_2^2, \quad (7)$$

$$\tilde{\mathcal{L}}_\theta(\mathbf{x}_t, t, \phi, \psi) = \omega(t) \frac{a_t^2}{\sigma_t^4} (f_{\phi, \kappa_4}(\mathbf{x}_t, t, \mathbf{c}) - f_{\psi, \kappa_2}(\mathbf{x}_t, t, \mathbf{c}))^T (f_{\psi, \kappa_3}(\mathbf{x}_t, t, \mathbf{c}) - \mathbf{x}_g). \quad (8)$$

2.3 Long and Short Guidance

Previous works equipped with a fake score network f_ψ typically only consider adding CFG when evaluating the pretrained score network f_ϕ , such as in DMD [Yin et al., 2023]. In the context of SiD, this corresponds to setting $\kappa_1 = \kappa_2 = \kappa_3 = 1$ and $\kappa_4 > 1$. In this paper, we discover that a broad spectrum of combinations of $\kappa_1, \kappa_2, \kappa_3$, and κ_4 can all significantly enhance performance compared to not using any CFG at all. These settings are found to lead to different balances of minimizing FID, which reflects how well the generated data match the training data in distribution,

and maximizing the CLIP score [Radford et al., 2021], which reflects how well the generated images follow the textual guidance.

This flexibility to accommodate various CFG combinations expands the design space for SD distillation, balancing generation quality and text adherence. However, given the vastness of the search space, we are motivated to develop strategies that constrain the scope of exploration.

Long strategy: Enhancing CFG of the pretrained score network f_ϕ . Aligning with established practices, the most fundamental approach involves enhancing the CFG of the pretrained score network f_ϕ . An example setting under this strategy in SiD is: $\kappa_1 = \kappa_2 = \kappa_3 = 1$ and $\kappa_4 = 3$. The rationale is that by biasing the teacher network f_ϕ to favor generations more aligned with c using a CFG scale of $\kappa_4 = 3$, the student generator is compelled to follow suit. We will present experimental results to demonstrate the effectiveness of this strategy while also discussing its limitations.

Short strategy: Weakening CFG of the fake score network f_ψ . With the availability of a fake score network f_ψ , we have developed a new strategy to enhance SiD’s text-to-image generation capabilities by reducing the CFG of f_ψ in SiD. An exemplary configuration is setting $\kappa_1 = \kappa_4 = 1$ while allowing $\kappa_2 = \kappa_3$ to vary within $(0, 1)$. The underlying idea is that by diminishing f_ψ ’s capacity to detect generations aligned with c through a reduced CFG scale ($0 < \kappa_2 < 1$), the student generator is incentivized to produce images that better align with the textual guidance to compensate for this reduction. We will present experiments to assess the efficacy and limitations of this strategy.

Long and short CFGs. We introduce an innovative strategy termed long-short guidance (LSG), where we enhance CFG during the training of f_ψ by setting $\kappa_1 > 1$, and maintain CFGs on f_ψ and f_ϕ during the training of G_θ at the same or a lower scale by setting $1 \leq \kappa_2 = \kappa_3 = \kappa_4 \leq \kappa_1$. The logic behind this approach is that enhancing the CFG of f_ψ during training effectively reduces the CFG at evaluation time when used at the same or a reduced level. To our knowledge, we are the first to incorporate CFG into the training of the fake score network. LSG has been found to achieve a better balance between FID and CLIP scores, optimizing performance across these metrics.

3 Experiments

We summarize the parameter settings, such as batch size, learning rate, and optimizer configurations, in Table 3 in Appendix C. Unless specified in ablation studies, the settings are uniformly applied across all guidance strategies. We present the details of our method in Algorithm 1, where we generate an image in one step and generalize the setting in DMD and SiD to set $\omega(t)$ as

$$\mathbf{x}_g = G_\theta(\mathbf{z}, \mathbf{c}) = f_\theta(\sigma_{t_{init}} \mathbf{z}, t_{init}, \mathbf{c}), \quad \mathbf{z} \sim \mathcal{N}(0, \mathbf{I}); \quad \omega(t) = \frac{\sigma_t^4}{a_t^2} \frac{C}{\|\mathbf{x}_g - f_{\phi, \kappa_4}(\mathbf{x}_t, t, \mathbf{c})\|_{1, sg}}, \quad (9)$$

where C is the total number of pixels in \mathbf{x}_g . We initialize both ψ and θ using the pretrained ϕ from SD. We have performed an ablation study that chooses $t_{init} \in \{354, 550, 625, 675, 800, 900, 999\}$ and found that the model’s performance under FP32 optimization is not sensitive to these choices. To align with the setting in SiD, we set $t_{init} = 625$, which would result in $\sigma_{t_{init}}/a_{t_{init}} = 2.5$ under the DDPM schedule used to train SD1.5. We conduct a comprehensive study to evaluate the performance of SiD using the proposed LSG for distilling SD1.5. Additionally, we apply the same LSG scales to distill SD2.1-base, further assessing the adaptability and effectiveness of our approach across different model versions.

We consider a standard setting that utilizes the Aesthetics6+ prompt [Cherti et al., 2023] for training and evaluates performance by computing zero-shot FID on the COCO-2014 validation set. We adhere to the standard protocol by generating 30k images to compare with the 40,504 images in the COCO-2014 validation set for calculating zero-shot FID. Additionally, we employ the ViT-g-14-1a1on2b_s12b_b42k encoder [Ilharco et al., 2021, Cherti et al., 2023] to compute the CLIP score [Radford et al., 2021]. The FID and CLIP scores presented in the figures are calculated using randomly sampled prompts from the COCO-2014 validation set. When reporting the FID and CLIP results of SiD in Table 1, we follow DMD [Yin et al., 2023] to use the exact evaluation code¹ provided by GigaGAN [Kang et al., 2023], where a pre-defined list of 30k text prompts selected from the COCO-2014 validation set is used to generate the 30k images, which are used for computing FID and CLIP scores with images from the validation set as the reference.

¹<https://github.com/mingukang/GigaGAN/tree/main/evaluation>

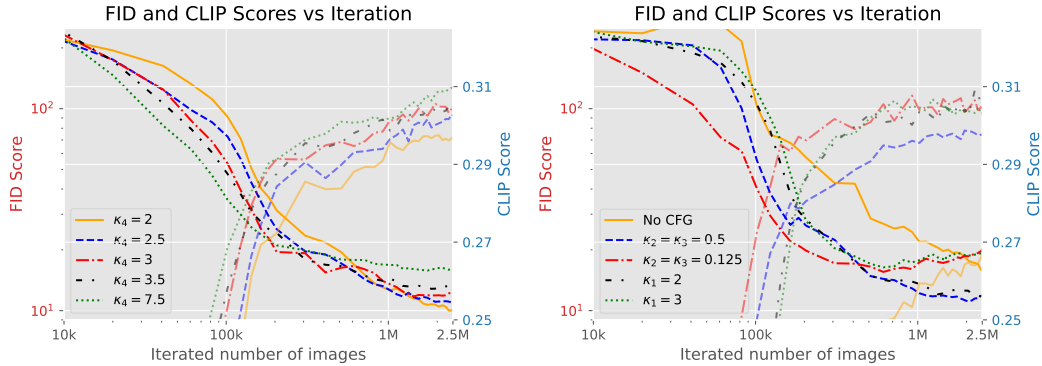


Figure 3: **Left (Long CFG of the true score network):** This plot illustrates the progression of FID and CLIP scores, each influenced by different CFGs applied to the true score network. The κ 's not specified in the legends are set as 1. FID scores are plotted on the primary y-axis, while CLIP scores are displayed on the secondary y-axis in corresponding line styles but with slight transparency. Together, these lines demonstrate how various CFGs impact model performance. **Right (Short CFG of the fake score network):** Analogous plot to the left where the CFGs of the fake score network are either weakened during evaluation or enhanced during training.

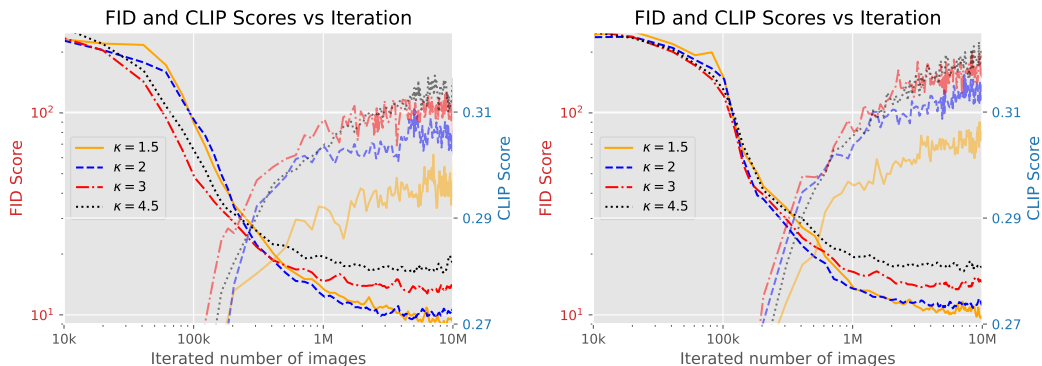


Figure 4: The plot with the proposed long-short guidance (LSG) demonstrates the FID and CLIP progressions of SiD in SD1.5 (left panel) and SD2.1-base (right panel).

3.1 Long and/or short guidance strategies

Long the CFG of the pretrained score network. For the long strategy, we set $\kappa_1 = \kappa_2 = \kappa_3 = 1$ and $\kappa_4 > 1$, specifically exploring values of κ_4 from the set $\{2, 2.5, 3, 3.5, 7.5\}$. As shown in the left panel of Figure 3, our experiments results indicate that this setup yields highly competitive performance, even after processing as few as 2.5 million fake images (approximately 5,000 iterations with a mini-batch size of 512). The parameter κ_4 plays a crucial role in balancing FID and CLIP scores. For achieving lower FID scores, $\kappa_4 = 2$ can yield an FID close to 10, while for higher CLIP scores, $\kappa_4 = 7.5$ can result in a CLIP score around 0.31. However, our primary objective is to devise a strategy that lowers FID while minimizing CLIP degradation.

Short the CFG of the fake score network. For the short strategy, we set $\kappa_1 = \kappa_4 = 1$ and explore $\kappa_2 = \kappa_3 \in \{0.5, 0.125\}$. As illustrated in the right panel of Figure 3, this approach delivers competitive performance, with κ_2 dictating the balance between FID and CLIP scores. However, compared to the long strategy, this configuration generally produces inferior results, as suggested by lower CLIP scores when FIDs are controlled to similar levels. From this figure, it's also evident that when No CFG is employed, where $\kappa_1 = \kappa_2 = \kappa_3 = \kappa_4 = 1$, the results are underwhelming, underscoring the importance of injecting CFGs into SiD to distill text-to-image diffusion models.

LSG: Long and Short classifier-free Guidance. LSG is an innovative strategy that enhances the performance of SiD in text-guided diffusion distillation. In the simplest LSG configuration, we amplify the CFG during the training of f_ψ , the fake score network, and reduce it during the training of G_θ , the one-step generator. Specifically, to long the CFG of f_ψ during its training while shorting it during its evaluation, we set κ_1 as 2 or 3 and set $\kappa_2 = \kappa_3 = \kappa_4 = 1$. As depicted in the right panel of

Table 1: Comparison of image generation methods across various metrics. Inference times are estimated using a Nvidia A100 GPU as reference. The numbers of the methods marked with † are produced by running the publicly available model checkpoints. Other data are sourced from corresponding scientific papers with comparisons as reported. The value followed by symbol \sim indicates it is estimated based on the plots shown in the paper.

| Method | Res. | Time (\downarrow) | # Steps | # Param. | FID (\downarrow) | CLIP (\uparrow) |
|--|------|-----------------------|---------|----------|----------------------|---------------------|
| Autoregressive Models | | | | | | |
| DALL·E [Ramesh et al., 2021] | 256 | - | - | 12B | 27.5 | - |
| CogView2 | 256 | - | - | 6B | 24.0 | - |
| Parti-750M [Yu et al., 2022] | 256 | - | - | 750M | 10.71 | - |
| Parti-3B [Yu et al., 2022] | 256 | 6.4s | - | 3B | 8.10 | - |
| Parti-20B [Yu et al., 2022] | 256 | - | - | 20B | 7.23 | - |
| Make-A-Scene [Gafni et al., 2022] | 256 | 25.0s | - | - | 11.84 | - |
| Masked Models | | | | | | |
| Muse [Chang et al., 2023] | 256 | 1.3 | 24 | 3B | 7.88 | 0.32 |
| Diffusion Models | | | | | | |
| GLIDE [Nichol et al., 2022] | 256 | 15.0s | 250 | 5B | 12.24 | - |
| DALL·E 2 [Ramesh et al., 2022] | 256 | - | 250+27 | 5.5B | 10.39 | - |
| LDM [Rombach et al., 2022] | 256 | 3.7s | 250 | 1.45B | 12.63 | - |
| Imagen [Ho et al., 2022] | 256 | 9.1s | - | 3B | 7.27 | - |
| eDiff-I [Balaji et al., 2022] | 256 | 32.0s | 25+10 | 9B | 6.95 | - |
| Generative Adversarial Networks (GANs) | | | | | | |
| LAFITE [Zhou et al., 2022] | 256 | 0.02s | 1 | 75M | 26.94 | - |
| StyleGAN-T [Sauer et al., 2023a] | 512 | 0.10s | 1 | 1B | 13.90 | \sim 0.293 |
| GigaGAN [Kang et al., 2023] | 512 | 0.13s | 1 | 1B | 9.09 | - |
| Distilled Stable Diffusion 2.1 | | | | | | |
| †ADD (SD-Turbo) [Sauer et al., 2023b] | 512 | - | 1 | - | 16.25 | 0.335 |
| Distilled Stable Diffusion XL | | | | | | |
| †ADD (SDXL-Turbo) [Sauer et al., 2023b] | 512 | - | 1 | - | 19.08 | 0.343 |
| Stable Diffusion 1.5 and its accelerated or distilled versions | | | | | | |
| SD1.5 (CFG=3) [Rombach et al., 2022] | 512 | 2.59s | 250 | 0.9B | 8.78 | - |
| SD1.5 (CFG=7.5) [Rombach et al., 2022] | 512 | 2.59s | 250 | 0.9B | 13.45 | 0.322 |
| DPM++ (4 step) [Lu et al., 2022a] | 512 | 0.26s | 4 | 0.9B | 22.44 | 0.31 |
| UniPC (4 step) [Zhao et al., 2023] | 512 | 0.26s | 4 | 0.9B | 22.30 | 0.31 |
| LCM-LoRA (4 step) [Luo et al., 2023b] | 512 | 0.19s | 4 | 0.9B | 23.62 | 0.30 |
| LCM-LoRA (1 step) [Luo et al., 2023b] | 512 | 0.07s | 1 | 0.9B | 77.90 | 0.24 |
| InstaFlow-0.9B [Liu et al., 2023] | 512 | 0.09s | 1 | 0.9B | 13.10 | 0.28 |
| InstaFlow-1.7B [Liu et al., 2023] | 512 | 0.12s | 1 | 1.7B | 11.83 | - |
| UFOGen [Xu et al., 2023] | 512 | 0.09s | 1 | 0.9B | 12.78 | - |
| DMD (CFG=3) [Yin et al., 2023] | 512 | 0.09s | 1 | 0.9B | 11.49 | 0.32 |
| DMD (CFG=8) [Yin et al., 2023] | 512 | 0.09s | 1 | 0.9B | 14.93 | 0.32 |
| BOOT [Gu et al., 2023] | 512 | 0.09s | 1 | 0.9B | 48.20 | 0.26 |
| Guided Distillation [Meng et al., 2023] | 512 | - | 1 | 0.9B | 37.3 | 0.27 |
| SiD-LSG ($\kappa = 1.5$) | 512 | 0.09s | 1 | 0.9B | 8.71 | 0.302 |
| SiD-LSG ($\kappa = 1.5$, double the training time) | 512 | 0.09s | 1 | 0.9B | 8.15 | 0.304 |
| SiD-LSG ($\kappa = 2$) | 512 | 0.09s | 1 | 0.9B | 9.56 | 0.313 |
| SiD-LSG ($\kappa = 3$) | 512 | 0.09s | 1 | 0.9B | 13.21 | 0.314 |
| SiD-LSG ($\kappa = 4.5$) | 512 | 0.09s | 1 | 0.9B | 16.59 | 0.317 |
| Stable Diffusion 2.1-base and its distilled versions | | | | | | |
| SD2.1-base [Rombach et al., 2022] | 512 | 0.09s | 1 | 0.9B | 202.14 | 0.08 |
| SD2.1 base [Rombach et al., 2022] | 512 | 0.77s | 25 | 0.9B | 13.45 | 0.30 |
| SwiftBrush [Nguyen and Tran, 2024] | 512 | 0.09 | 1 | 0.9B | 16.67 | 0.29 |
| SiD-LSG ($\kappa = 1.5$) | 512 | 0.09s | 1 | 0.9B | 9.52 | 0.308 |
| SiD-LSG ($\kappa = 2$) | 512 | 0.09s | 1 | 0.9B | 10.97 | 0.318 |
| SiD-LSG ($\kappa = 3$) | 512 | 0.09s | 1 | 0.9B | 13.50 | 0.321 |
| SiD-LSG ($\kappa = 4.5$) | 512 | 0.09s | 1 | 0.9B | 16.54 | 0.322 |

Figure 3, setting $\kappa_1 = 3$ (green lines) is as effective as the short strategy with $\kappa_2 = \kappa_3 = 0.125$ (red lines), and $\kappa_1 = 2$ (black lines) outperforms the short strategy with $\kappa_2 = \kappa_3 = 0.5$ (blue lines) and is comparable to the long strategy with $\kappa_4 = 3$ (red lines in the left panel). These results validate LSG as an effective guidance strategy to boost SiD’s performance in text-guided diffusion distillation.

Nevertheless, merely matching the best long or short strategy does not suffice to advocate for LSG. However, the performance notably improves if maintaining the CFG scale of the fake score network

Table 2: Comparison of HPSv2 score and Precision/Recall on the COCO-2014 validation set. The HPSv2 scores of ADD (SD-Turbo) are produced based on the publicly available model checkpoint. The HPSv2 scores of the other baselines are quoted from SwiftBrush [Nguyen and Tran, 2024]. The Precision and Recall on COCO-2014 are obtained using the 30K images generated by the corresponding model checkpoints. The SwiftBrush checkpoint was provided upon request by the authors.

| Teacher | Student | Human Preference Score v2 \uparrow | | | | COCO-2014 Precision and Recall \uparrow | |
|------------|--|--------------------------------------|--------------|--------------|--------------|---|-------------|
| | | Anime | Photo | Concept Art | Paintings | Precision | Recall |
| SD2.1 | ADD (SD-Turbo) [Sauer et al., 2023b] | 27.48 | 26.89 | 26.86 | 27.46 | 0.65 | 0.35 |
| SD1.5 | LCM [Luo et al., 2023b] | 22.61 | 22.71 | 22.74 | 22.91 | - | - |
| SD1.5 | InstaFlow [Liu et al., 2023] | 25.98 | 26.32 | 25.79 | 25.93 | 0.53 | 0.45 |
| SD1.5 | BOOT [Gu et al., 2023] | 25.29 | 25.16 | 24.40 | 24.61 | - | - |
| SD2.1-base | SwiftBrush [Nguyen and Tran, 2024] | 26.91 | 27.21 | 26.32 | 26.37 | 0.47 | 0.46 |
| SD1.5 | SiD-LSG ($\kappa = 1.5$) | 26.58 | 26.80 | 26.02 | 26.02 | 0.59 | 0.52 |
| | SiD-LSG ($\kappa = 1.5$, double the training time) | 26.58 | 26.80 | 26.01 | 26.02 | 0.60 | 0.53 |
| | SiD-LSG ($\kappa = 2$) | 26.94 | 27.03 | 26.35 | 26.27 | 0.64 | 0.48 |
| | SiD-LSG ($\kappa = 3$) | 27.10 | 27.11 | 26.47 | 26.46 | 0.65 | 0.40 |
| | SiD-LSG ($\kappa = 4.5$) | 27.39 | 27.30 | 26.65 | 26.58 | 0.67 | 0.34 |
| SD2.1-base | SiD-LSG ($\kappa = 1.5$) | 26.65 | 26.87 | 26.19 | 26.14 | 0.60 | 0.49 |
| | SiD-LSG ($\kappa = 2$) | 26.90 | 27.08 | 26.43 | 26.47 | 0.62 | 0.44 |
| | SiD-LSG ($\kappa = 3$) | 27.27 | 27.22 | 26.75 | 26.72 | 0.64 | 0.38 |
| | SiD-LSG ($\kappa = 4.5$) | 27.42 | 27.31 | 26.81 | 26.79 | 0.63 | 0.34 |

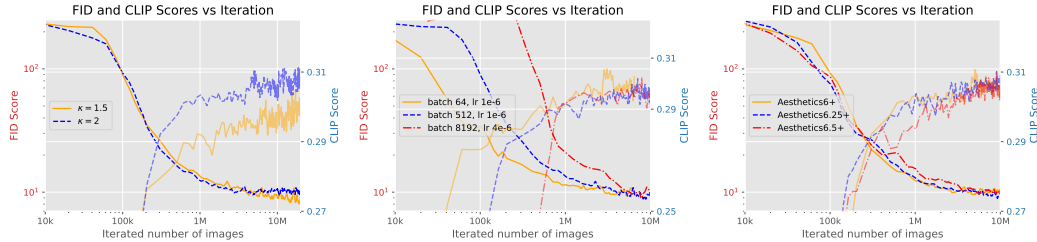


Figure 5: This figure illustrates the progression of FID and CLIP scores during an ablation study of distilling SD1.5 using SiD-LSG. The default settings of batch size 512, learning rate 1e-6, LSG scale 2, and Prompt Aesthetics6+ are maintained unless specified otherwise. **Left:** The number of training fake images is doubled from 10M to 20M under LSG scales of 1.5 and 2.0. **Middle:** Variations in batch size and learning rate settings under LSG 1.5. **Right:** Comparison of training prompts Aesthetics6+, Aesthetics6.25+, and Aesthetics6.5+.

during the generator’s training after initially increasing it during its own training , effectively balancing FID minimization and CLIP maximization. We explore $\kappa_1 = \kappa_2 = \kappa_3 = \kappa_4$ within $\{1.5, 2, 3, 4.5\}$, and present the results in Figure 4 for distilling both SD 1.5 and 2.1-base. Comparisons between SD1.5 outcomes in the left panel of Figure 4 and those in Figure 3 demonstrate superior performance with this LSG setting, indicated by higher CLIP scores at controlled FID levels, and lower FID scores at controlled CLIP levels. Generally, within the range of 1.5 to 4.5, a lower guidance scale correlates with better FID but worse CLIP, and vice versa, as evidenced by the curves for both SD 1.5 and 2.1-base in Figure 4.

3.2 Ablation study

We investigate the impact of extended training durations under two different guidance scales, variations in batch size, and the selection of training prompts. Initially, we doubled the number of fake images used to train the generator from 10M to 20M and monitored the evolution of the FID and CLIP scores. From the left panel of Figure 5, we observe continuous improvements in both FID and CLIP scores for an LSG of 1.5 when training is extended beyond 10M fake images, and sustained enhancements in CLIP scores for an LSG of 2.0. Notably, by doubling the training input from 10M to 20M fake images, the FID under LSG 1.5 decreased from 8.71 to a record low of **8.15** among diffusion distillation methods.

Additionally, we assessed the effects of batch size by considering two additional settings: a batch size of 8192 with a learning rate of 4e-6, a configuration used in SiD to distill the EDM model pretrained on ImageNet 64x64 [Zhou et al., 2024], and a batch size of 64 with a learning rate of 1e-6. The middle panel of Figure 5 demonstrates that while there are initial differences in the convergence speed in terms of the number of fake images processed, the performances eventually converge to similar levels. We note that while smaller batch sizes may seem to converge faster, they require more time to process the same number of images. This is due to more frequent model parameter

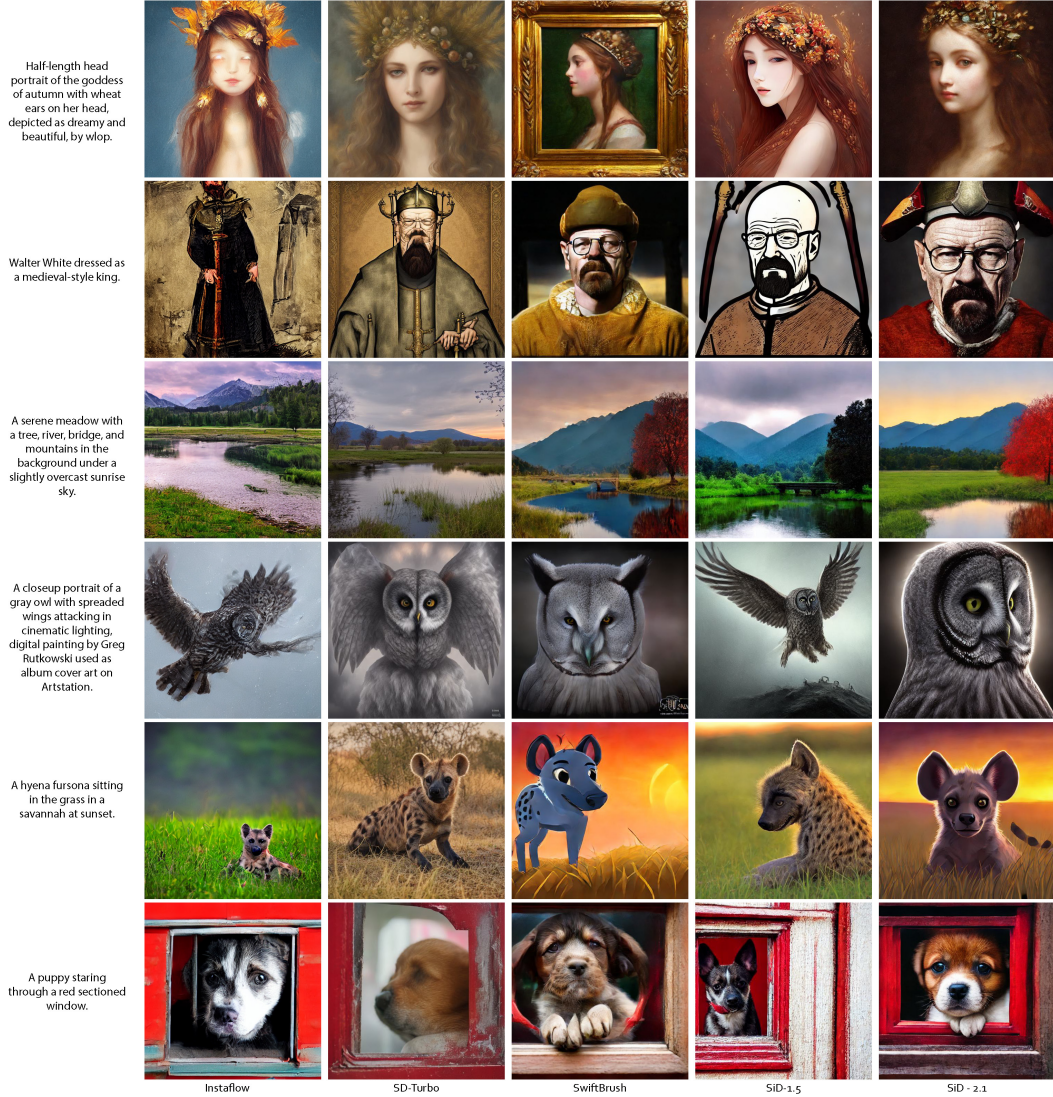


Figure 6: Qualitative comparison of one-step distillation methods using identical text prompts and random seeds.

updates, higher communication costs between GPUs, and additional overheads typically associated with smaller batch sizes.

Lastly, we explored the effect of changing training prompts, shifting from the Aesthetics6+ prompts to Aesthetics6.25+ and Aesthetics6.5+ prompts [Cherti et al., 2023]. The performance, as shown in the right panel of Figure 5, appears comparable across these variations. Specifically, under an LSG of 2.0, switching from Aesthetics6+ to Aesthetics6.25+ enabled us to further reduce the FID from the 9.56 reported in Table 1 to 9.21, although the CLIP score decreased slightly from 0.313 to 0.311, indicating no significant performance disparity between them.

The results of the ablation study show that SiD-LSG has low sensitivity to variations in batch size and training prompts and its performance could potentially be further enhanced with extended training.

3.3 Quantitative and qualitative evaluations

We present comprehensive results from prior studies across various experimental settings, including both one-step and multi-step generation methods. When evaluation results are available in existing literature [Yin et al., 2023, Liu et al., 2023, Kang et al., 2023, Nguyen and Tran, 2024], we directly cite them; otherwise, if model checkpoints are accessible, either publicly or provided upon request by

the authors, we utilize the evaluation code from GigaGAN to produce the reported results. For our SiD-LSG, we select $\kappa_1 = \kappa_2 = \kappa_3 = \kappa_4 \in \{1.5, 2.0, 3.0, 4.5\}$.

For comparisons of FID and CLIP scores, the results are detailed in Table 1. Among all one-step distillation methods, our approach notably excels in zero-shot text-conditioned image generation on the COCO-2014 dataset, as reflected by both FID-30K and CLIP scores. Specifically, with the guidance scale set as 2, our method attains FID scores as low as 9.56 and 10.97, and a CLIP score above 0.31 and around 0.32, using SD 1.5 and 2.1-base as the pretrained backbones, respectively. Notably, by setting the guidance scale to 1.5 and doubling the training time, our data-free method achieves a record-low FID of **8.15**, along with a CLIP score of 0.304, when distilling SD1.5. These results remain highly competitive when compared to other generative approaches, such as autoregressive models and GANs, and are even comparable to previous multi-step diffusion-based sampling methods. Analyzing different κ values, we observe a trade-off between FID and CLIP scores: smaller κ values generally yield better FID metrics, while larger values enhance CLIP scores, aligning with past findings on the impact of guidance scale.

Beyond FID and CLIP scores, we also assess Precision and Recall [Kynkäänniemi et al., 2019] as well as Human Preference Score (HPSv2) [Wu et al., 2023], which are presented in Table 2. We reuse the same 30k images from previous evaluations for the Precision and Recall calculations. For HPSv2, we follow their established protocol, generating images from 800 text prompts per category. Our SiD-LSG models outperform other baselines in HPSv2 scores across all categories, as well as in Precision and Recall metrics. Notably, with $\kappa = 4.5$, SiD-LSG reaches peak performance in distilling SD2.1-base. Regarding Precision and Recall, higher κ values lead to improved Precision, while lower values result in better Recall.

For qualitative verification, we utilize our models with $\kappa = 4.5$, selecting six prompts from across all HPSv2 categories to generate images. To ensure a fair comparison, we maintain the same random seed for image generation across all methods. The visual results are illustrated in Figure 6, where SiD consistently shows superior text-image alignment and visual fidelity.

For broader impact, please refer to the discussion in Appendix A. For limitations and computational requirements, please refer to a detailed discussion in Appendix D.

4 Conclusion

In this paper, we introduce a novel method that integrates Classifier-Free Guidance (CFG) with Score identity Distillation (SiD) to efficiently distill Stable Diffusion models into effective one-step generators. Utilizing our innovative long and short CFG strategies (LSG), we have successfully distilled these models using only fake images synthesized by the one-step generator itself. Our approach not only demonstrates the practical potential of SiD, but also sets new benchmarks for one-step diffusion distillation in zero-shot FID scores on the COCO-2014 validation set. The anticipated release of our tools and models is expected to make a significant impact on research and development in generative modeling. This release is designed to enhance efficiency without compromising performance, and it facilitates learning from the teacher model without the need for real images or the addition of extra regression or adversarial losses.

Acknowledgments and Disclosure of Funding

We are grateful for the contributions of Michael (Qijia) Zhou in preparing the data and code. We also extend our thanks to Tianwei Yin for clarifying our queries regarding the evaluation protocol of DMD on FID and CLIP scores. Additionally, we appreciate Thuan Hoang Nguyen for responding to our questions about SwiftBrush and for kindly providing a model checkpoint upon request. M. Zhou, H. Zheng, and Z. Wang acknowledge the support of NSF-IIS 2212418 and NIH-R37 CA271186.

References

Josh Achiam, Steven Adler, Sandhini Agarwal, Lama Ahmad, Ilge Akkaya, Florencia Leoni Aleman, Diogo Almeida, Janko Altenschmidt, Sam Altman, Shyamal Anadkat, et al. GPT-4 technical report. *arXiv preprint arXiv:2303.08774*, 2023.

- Michael S Albergo, Nicholas M Boffi, and Eric Vanden-Eijnden. Stochastic interpolants: A unifying framework for flows and diffusions. *arXiv preprint arXiv:2303.08797*, 2023.
- Jacob Austin, Daniel D Johnson, Jonathan Ho, Daniel Tarlow, and Rianne van den Berg. Structured denoising diffusion models in discrete state-spaces. *Advances in Neural Information Processing Systems*, 34:17981–17993, 2021.
- Yogesh Balaji, Seungjun Nah, Xun Huang, Arash Vahdat, Jiaming Song, Qinsheng Zhang, Karsten Kreis, Miika Aittala, Timo Aila, Samuli Laine, Bryan Catanzaro, Tero Karras, and Ming-Yu Liu. eDiff-I: Text-to-image diffusion models with an ensemble of expert denoisers. *arXiv preprint arXiv:2211.01324*, 2022.
- Tom Brown, Benjamin Mann, Nick Ryder, Melanie Subbiah, Jared D Kaplan, Prafulla Dhariwal, Arvind Neelakantan, Pranav Shyam, Girish Sastry, Amanda Askell, Sandhini Agarwal, Ariel Herbert-Voss, Gretchen Krueger, Tom Henighan, Rewon Child, Aditya Ramesh, Daniel Ziegler, Jeffrey Wu, Clemens Winter, Chris Hesse, Mark Chen, Eric Sigler, Mateusz Litwin, Scott Gray, Benjamin Chess, Jack Clark, Christopher Berner, Sam McCandlish, Alec Radford, Ilya Sutskever, and Dario Amodei. Language models are few-shot learners. *Advances in neural information processing systems*, 33:1877–1901, 2020.
- Huiwen Chang, Han Zhang, Jarred Barber, Aaron Maschinot, Jose Lezama, Lu Jiang, Ming-Hsuan Yang, Kevin Patrick Murphy, William T. Freeman, Michael Rubinstein, Yuanzhen Li, and Dilip Krishnan. Muse: Text-to-image generation via masked generative transformers. In Andreas Krause, Emma Brunskill, Kyunghyun Cho, Barbara Engelhardt, Sivan Sabato, and Jonathan Scarlett, editors, *Proceedings of the 40th International Conference on Machine Learning*, volume 202 of *Proceedings of Machine Learning Research*, pages 4055–4075. PMLR, 23–29 Jul 2023. URL <https://proceedings.mlr.press/v202/chang23b.html>.
- Soravit Changpinyo, Piyush Sharma, Nan Ding, and Radu Soricut. Conceptual 12M: Pushing web-scale image-text pre-training to recognize long-tail visual concepts. In *CVPR*, 2021.
- Tianqi Chen and Mingyuan Zhou. Learning to Jump: Thinning and thickening latent counts for generative modeling. In *ICML 2023: International Conference on Machine Learning*, July 2023. URL <http://arxiv.org/abs/2305.18375>.
- Mehdi Cherti, Romain Beaumont, Ross Wightman, Mitchell Wortsman, Gabriel Ilharco, Cade Gordon, Christoph Schuhmann, Ludwig Schmidt, and Jenia Jitsev. Reproducible scaling laws for contrastive language-image learning. In *Proceedings of the IEEE/CVF Conference on Computer Vision and Pattern Recognition*, pages 2818–2829, 2023.
- Wang Chong, David Blei, and Fei-Fei Li. Simultaneous image classification and annotation. In *2009 IEEE Conference on computer vision and pattern recognition*, pages 1903–1910. IEEE, 2009.
- Jacob Devlin, Ming-Wei Chang, Kenton Lee, and Kristina Toutanova. BERT: Pre-training of deep bidirectional transformers for language understanding. *arXiv preprint arXiv:1810.04805*, 2018.
- Prafulla Dhariwal and Alexander Nichol. Diffusion models beat GANs on image synthesis. *Advances in Neural Information Processing Systems*, 34:8780–8794, 2021.
- Ming Ding, Zhuoyi Yang, Wenyi Hong, Wendi Zheng, Chang Zhou, Da Yin, Junyang Lin, Xu Zou, Zhou Shao, Hongxia Yang, et al. Cogview: Mastering text-to-image generation via transformers. *Advances in Neural Information Processing Systems*, 34:19822–19835, 2021.
- Patrick Esser, Robin Rombach, and Bjorn Ommer. Taming transformers for high-resolution image synthesis. In *Proceedings of the IEEE/CVF conference on computer vision and pattern recognition*, pages 12873–12883, 2021.
- Li Fei-Fei and Pietro Perona. A Bayesian hierarchical model for learning natural scene categories. In *2005 IEEE computer society conference on computer vision and pattern recognition (CVPR’05)*, volume 2, pages 524–531. IEEE, 2005.
- Oran Gafni, Adam Polyak, Oron Ashual, Shelly Sheynin, Devi Parikh, and Yaniv Taigman. Make-a-scene: Scene-based text-to-image generation with human priors. In *European Conference on Computer Vision*, pages 89–106. Springer, 2022.
- Ian Goodfellow, Jean Pouget-Abadie, Mehdi Mirza, Bing Xu, David Warde-Farley, Sherjil Ozair, Aaron Courville, and Yoshua Bengio. Generative adversarial nets. In *Advances in Neural Information Processing Systems*, pages 2672–2680, 2014.

- Karol Gregor, Ivo Danihelka, Alex Graves, Danilo Rezende, and Daan Wierstra. DRAW: A recurrent neural network for image generation. In *International conference on machine learning*, pages 1462–1471. PMLR, 2015.
- Jiatao Gu, Shuangfei Zhai, Yizhe Zhang, Lingjie Liu, and Joshua M Susskind. BOOT: Data-free distillation of denoising diffusion models with bootstrapping. In *ICML 2023 Workshop on Structured Probabilistic Inference and Generative Modeling*, 2023.
- Shuyang Gu, Dong Chen, Jianmin Bao, Fang Wen, Bo Zhang, Dongdong Chen, Lu Yuan, and Baining Guo. Vector quantized diffusion model for text-to-image synthesis. In *CVPR*, 2022.
- Pengcheng He, Xiaodong Liu, Jianfeng Gao, and Weizhu Chen. DeBERTa: Decoding-enhanced bert with disentangled attention. *arXiv preprint arXiv:2006.03654*, 2020.
- Martin Heusel, Hubert Ramsauer, Thomas Unterthiner, Bernhard Nessler, and Sepp Hochreiter. GANs trained by a two time-scale update rule converge to a local Nash equilibrium. In *Advances in Neural Information Processing Systems*, pages 6626–6637, 2017.
- G. Hinton, S. Osindero, and Y.-W. Teh. A fast learning algorithm for deep belief nets. *Neural Computation*, 18(7):1527–1554, 2006.
- Jonathan Ho and Tim Salimans. Classifier-free diffusion guidance. *arXiv preprint arXiv:2207.12598*, 2022.
- Jonathan Ho, Ajay Jain, and Pieter Abbeel. Denoising Diffusion Probabilistic Models. *Advances in Neural Information Processing Systems*, 33, 2020.
- Jonathan Ho, William Chan, Chitwan Saharia, Jay Whang, Ruiqi Gao, Alexey Gritsenko, Diederik P. Kingma, Ben Poole, Mohammad Norouzi, David J. Fleet, and Tim Salimans. Imagen video: High definition video generation with diffusion models. *arXiv preprint arXiv:2210.02303*, 2022.
- Chris C Holmes and Stephen G Walker. Assigning a value to a power likelihood in a general Bayesian model. *Biometrika*, 104(2):497–503, 2017.
- Emiel Hoogeboom, Didrik Nielsen, Priyank Jaini, Patrick Forré, and Max Welling. Argmax flows and multinomial diffusion: Learning categorical distributions. *Advances in Neural Information Processing Systems*, 34: 12454–12465, 2021.
- Minghui Hu, Yujie Wang, Tat-Jen Cham, Jianfei Yang, and Ponnuthurai N Suganthan. Global context with discrete diffusion in vector quantised modelling for image generation. In *Proceedings of the IEEE/CVF Conference on Computer Vision and Pattern Recognition*, pages 11502–11511, 2022.
- Gabriel Ilharco, Mitchell Wortsman, Ross Wightman, Cade Gordon, Nicholas Carlini, Rohan Taori, Achal Dave, Vaishaal Shankar, Hongseok Namkoong, John Miller, Hannaneh Hajishirzi, Ali Farhadi, and Ludwig Schmidt. Openclip, July 2021. URL <https://doi.org/10.5281/zenodo.5143773>. If you use this software, please cite it as below.
- Albert Q. Jiang, Alexandre Sablayrolles, Arthur Mensch, Chris Bamford, Devendra Singh Chaplot, Diego de las Casas, Florian Bressand, Gianna Lengyel, Guillaume Lample, Lucile Saulnier, Léo Renard Lavaud, Marie-Anne Lachaux, Pierre Stock, Teven Le Scao, Thibaut Lavril, Thomas Wang, Timothée Lacroix, and William El Sayed. Mistral 7B. *arXiv preprint arXiv:2310.06825*, 2023.
- Minguk Kang, Jun-Yan Zhu, Richard Zhang, Jaesik Park, Eli Shechtman, Sylvain Paris, and Taesung Park. Scaling up GANs for text-to-image synthesis. In *Proceedings of the IEEE/CVF Conference on Computer Vision and Pattern Recognition*, pages 10124–10134, 2023.
- Tero Karras, Samuli Laine, and Timo Aila. A style-based generator architecture for generative adversarial networks. In *Proceedings of the IEEE/CVF conference on computer vision and pattern recognition*, pages 4401–4410, 2019.
- Tero Karras, Miika Aittala, Timo Aila, and Samuli Laine. Elucidating the design space of diffusion-based generative models. In Alice H. Oh, Alekh Agarwal, Danielle Belgrave, and Kyunghyun Cho, editors, *Advances in Neural Information Processing Systems*, 2022. URL <https://openreview.net/forum?id=k7FuTOWM0c7>.
- Dongjun Kim, Chieh-Hsin Lai, Wei-Hsiang Liao, Naoki Murata, Yuhta Takida, Toshimitsu Uesaka, Yutong He, Yuki Mitsufuji, and Stefano Ermon. Consistency trajectory models: Learning probability flow ode trajectory of diffusion. *arXiv preprint arXiv:2310.02279*, 2023.

- Diederik P. Kingma and Max Welling. Auto-encoding variational Bayes. In *International Conference on Learning Representations*, 2014.
- Tuomas Kynkäänniemi, Tero Karras, Samuli Laine, Jaakko Lehtinen, and Timo Aila. Improved precision and recall metric for assessing generative models. *Advances in neural information processing systems*, 32, 2019.
- Benjamin Lefaudeux, Francisco Massa, Diana Liskovich, Wenhan Xiong, Vittorio Caggiano, Sean Naren, Min Xu, Jieru Hu, Marta Tintore, Susan Zhang, Patrick Labatut, Daniel Haziza, Luca Wehrstedt, Jeremy Reizenstein, and Grigory Sizov. xFormers: A modular and hackable Transformer modelling library. <https://github.com/facebookresearch/xformers>, 2022.
- Tsung-Yi Lin, Michael Maire, Serge Belongie, James Hays, Pietro Perona, Deva Ramanan, Piotr Dollár, and C Lawrence Zitnick. Microsoft coco: Common objects in context. In *European conference on computer vision*, pages 740–755. Springer, 2014.
- Yaron Lipman, Ricky TQ Chen, Heli Ben-Hamu, Maximilian Nickel, and Matt Le. Flow matching for generative modeling. *arXiv preprint arXiv:2210.02747*, 2022.
- Luping Liu, Yi Ren, Zhijie Lin, and Zhou Zhao. Pseudo numerical methods for diffusion models on manifolds. In *International Conference on Learning Representations*, 2022a. URL <https://openreview.net/forum?id=PLKWVd2yBkY>.
- Xingchao Liu, Chengyue Gong, and Qiang Liu. Flow straight and fast: Learning to generate and transfer data with rectified flow. *arXiv preprint arXiv:2209.03003*, 2022b.
- Xingchao Liu, Xiwen Zhang, Jianzhu Ma, Jian Peng, and Qiang Liu. InstafLOW: One step is enough for high-quality diffusion-based text-to-image generation. *arXiv preprint arXiv:2309.06380*, 2023.
- Cheng Lu, Yuhao Zhou, Fan Bao, Jianfei Chen, Chongxuan Li, and Jun Zhu. DPM-Solver++: Fast solver for guided sampling of diffusion probabilistic models. In *arXiv preprint arXiv:2211.01095*, 2022a.
- Cheng Lu, Yuhao Zhou, Fan Bao, Jianfei Chen, Chongxuan Li, and Jun Zhu. DPM-solver: A fast ODE solver for diffusion probabilistic model sampling in around 10 steps. In Alice H. Oh, Alekh Agarwal, Danielle Belgrave, and Kyunghyun Cho, editors, *Advances in Neural Information Processing Systems*, 2022b. URL https://openreview.net/forum?id=2uAaGw1P_V.
- Eric Luhman and Troy Luhman. Knowledge distillation in iterative generative models for improved sampling speed. *arXiv preprint arXiv:2101.02388*, 2021.
- Simian Luo, Yiqin Tan, Longbo Huang, Jian Li, and Hang Zhao. Latent consistency models: Synthesizing high-resolution images with few-step inference. *ArXiv*, abs/2310.04378, 2023a.
- Simian Luo, Yiqin Tan, Suraj Patil, Daniel Gu, Patrick von Platen, Apolinário Passos, Longbo Huang, Jian Li, and Hang Zhao. Lcm-lora: A universal stable-diffusion acceleration module. *arXiv preprint arXiv:2310.04378*, 2023b.
- Weijian Luo, Tianyang Hu, Shifeng Zhang, Jiacheng Sun, Zhenguo Li, and Zhihua Zhang. Diff-Instruct: A universal approach for transferring knowledge from pre-trained diffusion models. In *Thirty-seventh Conference on Neural Information Processing Systems*, 2023c. URL <https://openreview.net/forum?id=MLIs5iRq4w>.
- Siwei Lyu. Interpretation and generalization of score matching. In *Proceedings of the Twenty-Fifth Conference on Uncertainty in Artificial Intelligence*, pages 359–366, 2009.
- Zhaoyang Lyu, Xudong Xu, Ceyuan Yang, Dahua Lin, and Bo Dai. Accelerating diffusion models via early stop of the diffusion process. *arXiv preprint arXiv:2205.12524*, 2022.
- Elman Mansimov, Emilio Parisotto, Jimmy Lei Ba, and Ruslan Salakhutdinov. Generating images from captions with attention. *arXiv preprint arXiv:1511.02793*, 2015.
- Chenlin Meng, Robin Rombach, Ruiqi Gao, Diederik Kingma, Stefano Ermon, Jonathan Ho, and Tim Salimans. On distillation of guided diffusion models. In *Proceedings of the IEEE/CVF Conference on Computer Vision and Pattern Recognition*, pages 14297–14306, 2023.
- Shakir Mohamed and Balaji Lakshminarayanan. Learning in implicit generative models. *arXiv preprint arXiv:1610.03483*, 2016.
- Thuan Hoang Nguyen and Anh Tran. SwiftBrush: One-step text-to-image diffusion model with variational score distillation. In *IEEE/CVF Conference on Computer Vision and Pattern Recognition (CVPR)*, 2024.

- Alexander Quinn Nichol, Prafulla Dhariwal, Aditya Ramesh, Pranav Shyam, Pamela Mishkin, Bob McGrew, Ilya Sutskever, and Mark Chen. Glide: Towards photorealistic image generation and editing with text-guided diffusion models. In *International Conference on Machine Learning*, pages 16784–16804. PMLR, 2022.
- Kushagra Pandey, Avideep Mukherjee, Piyush Rai, and Abhishek Kumar. DiffuseVAE: Efficient, controllable and high-fidelity generation from low-dimensional latents. *arXiv preprint arXiv:2201.00308*, 2022.
- George Papamakarios, Eric Nalisnick, Danilo Jimenez Rezende, Shakir Mohamed, and Balaji Lakshminarayanan. Normalizing flows for probabilistic modeling and inference. *arXiv preprint arXiv:1912.02762*, 2019.
- William Peebles and Saining Xie. Scalable diffusion models with transformers. In *Proceedings of the IEEE/CVF International Conference on Computer Vision*, pages 4195–4205, 2023.
- Dustin Podell, Zion English, Kyle Lacey, Andreas Blattmann, Tim Dockhorn, Jonas Müller, Joe Penna, and Robin Rombach. SDXL: Improving latent diffusion models for high-resolution image synthesis. In *The Twelfth International Conference on Learning Representations*, 2024. URL <https://openreview.net/forum?id=di52zR8xgf>.
- G. Polatkan, M. Zhou, L. Carin, D. Blei, and I. Daubechies. A Bayesian nonparametric approach to image super-resolution. *PAMI*, 37(2):346–358, 2015.
- Ben Poole, Ajay Jain, Jonathan T. Barron, and Ben Mildenhall. DreamFusion: Text-to-3D using 2D diffusion. *ArXiv*, abs/2209.14988, 2022.
- Can Qin, Shu Zhang, Ning Yu, Yihao Feng, Xinyi Yang, Yingbo Zhou, Huan Wang, Juan Carlos Niebles, Caiming Xiong, Silvio Savarese, et al. Unicontrol: A unified diffusion model for controllable visual generation in the wild. *arXiv preprint arXiv:2305.11147*, 2023.
- Alec Radford, Karthik Narasimhan, Tim Salimans, Ilya Sutskever, et al. Improving language understanding by generative pre-training. 2018.
- Alec Radford, Jeff Wu, Rewon Child, David Luan, Dario Amodei, and Ilya Sutskever. Language models are unsupervised multitask learners. 2019.
- Alec Radford, Jong Wook Kim, Chris Hallacy, Aditya Ramesh, Gabriel Goh, Sandhini Agarwal, Girish Sastry, Amanda Askell, Pamela Mishkin, Jack Clark, et al. Learning transferable visual models from natural language supervision. In *International conference on machine learning*, pages 8748–8763. PMLR, 2021.
- Colin Raffel, Noam Shazeer, Adam Roberts, Katherine Lee, Sharan Narang, Michael Matena, Yanqi Zhou, Wei Li, and Peter J Liu. Exploring the limits of transfer learning with a unified text-to-text transformer. *Journal of machine learning research*, 21(140):1–67, 2020.
- Aditya Ramesh, Mikhail Pavlov, Gabriel Goh, Scott Gray, Chelsea Voss, Alec Radford, Mark Chen, and Ilya Sutskever. Zero-shot text-to-image generation. In *International Conference on Machine Learning*, pages 8821–8831. PMLR, 2021.
- Aditya Ramesh, Prafulla Dhariwal, Alex Nichol, Casey Chu, and Mark Chen. Hierarchical text-conditional image generation with CLIP latents. *arXiv preprint arXiv:2204.06125*, 2022.
- Scott Reed, Zeynep Akata, Xinchun Yan, Lajanugen Logeswaran, Bernt Schiele, and Honglak Lee. Generative adversarial text to image synthesis. In *International conference on machine learning*, pages 1060–1069. PMLR, 2016.
- Danilo Jimenez Rezende, Shakir Mohamed, and Daan Wierstra. Stochastic backpropagation and approximate inference in deep generative models. In *Proceedings of the 31st International Conference on Machine Learning*, pages 1278–1286, 2014.
- Jason Tyler Rolfe. Discrete variational autoencoders. *arXiv preprint arXiv:1609.02200*, 2016.
- Robin Rombach, Andreas Blattmann, Dominik Lorenz, Patrick Esser, and Björn Ommer. High-resolution image synthesis with latent diffusion models. In *Proceedings of the IEEE/CVF conference on computer vision and pattern recognition*, pages 10684–10695, 2022.
- Chitwan Saharia, William Chan, Saurabh Saxena, Lala Li, Jay Whang, Emily L Denton, Kamyar Ghasemipour, Raphael Gontijo Lopes, Burcu Karagol Ayan, Tim Salimans, Jonathan Ho, David J Fleet, and Mohammad Norouzi. Photorealistic text-to-image diffusion models with deep language understanding. *Advances in Neural Information Processing Systems*, 35:36479–36494, 2022.

- Ruslan Salakhutdinov and Geoffrey Hinton. Deep Boltzmann machines. In *Artificial intelligence and statistics*, pages 448–455. PMLR, 2009.
- Tim Salimans and Jonathan Ho. Progressive distillation for fast sampling of diffusion models. In *International Conference on Learning Representations*, 2022. URL <https://openreview.net/forum?id=TIIdIXIpzhoI>.
- Axel Sauer, Katja Schwarz, and Andreas Geiger. StyleGAN-XL: Scaling StyleGAN to large diverse datasets. In *ACM SIGGRAPH 2022 conference proceedings*, pages 1–10, 2022.
- Axel Sauer, Tero Karras, Samuli Laine, Andreas Geiger, and Timo Aila. StyleGAN-T: Unlocking the power of GANs for fast large-scale text-to-image synthesis. *arXiv preprint arXiv:2301.09515*, 2023a.
- Axel Sauer, Dominik Lorenz, A. Blattmann, and Robin Rombach. Adversarial diffusion distillation. *ArXiv*, abs/2311.17042, 2023b.
- Christoph Schuhmann, Romain Beaumont, Richard Vencu, Cade Gordon, Ross Wightman, Mehdi Cherti, Theo Coombes, Aarush Katta, Clayton Mullis, Mitchell Wortsman, et al. LAION-5B: An open large-scale dataset for training next generation image-text models. *Advances in Neural Information Processing Systems*, 35: 25278–25294, 2022.
- Jascha Sohl-Dickstein, Eric Weiss, Niru Maheswaranathan, and Surya Ganguli. Deep unsupervised learning using nonequilibrium thermodynamics. In *International Conference on Machine Learning*, pages 2256–2265. PMLR, 2015.
- Jiaming Song, Chenlin Meng, and Stefano Ermon. Denoising diffusion implicit models. In *International Conference on Learning Representations*, 2021a. URL <https://openreview.net/forum?id=St1giarCHLP>.
- Yang Song and Prafulla Dhariwal. Improved techniques for training consistency models. *arXiv preprint arXiv:2310.14189*, 2023.
- Yang Song and Stefano Ermon. Generative Modeling by Estimating Gradients of the Data Distribution. In *Advances in Neural Information Processing Systems*, pages 11918–11930, 2019.
- Yang Song and Stefano Ermon. Improved Techniques for Training Score-Based Generative Models. *Advances in Neural Information Processing Systems*, 33, 2020.
- Yang Song, Conor Durkan, Iain Murray, and Stefano Ermon. Maximum likelihood training of score-based diffusion models. In *Advances in Neural Information Processing Systems (NeurIPS)*, 2021b.
- Yang Song, Jascha Sohl-Dickstein, Diederik P Kingma, Abhishek Kumar, Stefano Ermon, and Ben Poole. Score-based generative modeling through stochastic differential equations. In *International Conference on Learning Representations*, 2021c. URL <https://openreview.net/forum?id=PxtTIG12RRHS>.
- Yang Song, Prafulla Dhariwal, Mark Chen, and Ilya Sutskever. Consistency models. *arXiv preprint arXiv:2303.01469*, 2023.
- Bart Thomee, David A Shamma, Gerald Friedland, Benjamin Elizalde, Karl Ni, Douglas Poland, Damian Borth, and Li-Jia Li. YFCC100M: The new data in multimedia research. *Communications of the ACM*, 59(2):64–73, 2016.
- Hugo Touvron, Louis Martin, Kevin Stone, Peter Albert, Amjad Almahairi, Yasmine Babaei, Nikolay Bashlykov, Soumya Batra, Prajjwal Bhargava, Shruti Bhosale, et al. Llama 2: Open foundation and fine-tuned chat models. *arXiv preprint arXiv:2307.09288*, 2023.
- Dustin Tran, Rajesh Ranganath, and David Blei. Hierarchical implicit models and likelihood-free variational inference. In *Advances in Neural Information Processing Systems*, pages 5523–5533, 2017.
- Aaron van den Oord, Oriol Vinyals, and Koray Kavukcuoglu. Neural discrete representation learning. *Advances in neural information processing systems*, 30, 2017.
- Ashish Vaswani, Noam Shazeer, Niki Parmar, Jakob Uszkoreit, Llion Jones, Aidan N Gomez, Łukasz Kaiser, and Illia Polosukhin. Attention is all you need. *Advances in neural information processing systems*, 30, 2017.
- Pascal Vincent, Hugo Larochelle, Isabelle Lajoie, Yoshua Bengio, Pierre-Antoine Manzagol, and Léon Bottou. Stacked denoising autoencoders: Learning useful representations in a deep network with a local denoising criterion. *Journal of machine learning research*, 11(12), 2010.

- Zhendong Wang, Yifan Jiang, Yadong Lu, Pengcheng He, Weizhu Chen, Zhangyang Wang, Mingyuan Zhou, et al. In-context learning unlocked for diffusion models. *Advances in Neural Information Processing Systems*, 36:8542–8562, 2023a.
- Zhendong Wang, Huangjie Zheng, Pengcheng He, Weizhu Chen, and Mingyuan Zhou. Diffusion-GAN: Training GANs with diffusion. In *The Eleventh International Conference on Learning Representations*, 2023b. URL <https://openreview.net/forum?id=HZf7UbpWHuA>.
- Zhengyi Wang, Cheng Lu, Yikai Wang, Fan Bao, Chongxuan Li, Hang Su, and Jun Zhu. ProlificDreamer: High-fidelity and diverse text-to-3D generation with variational score distillation, 2023c.
- Xiaoshi Wu, Yiming Hao, Keqiang Sun, Yixiong Chen, Feng Zhu, Rui Zhao, and Hongsheng Li. Human Preference Score v2: A Solid Benchmark for Evaluating Human Preferences of Text-to-Image Synthesis. *arXiv preprint arXiv:2306.09341*, 2023.
- Zhisheng Xiao, Karsten Kreis, and Arash Vahdat. Tackling the generative learning trilemma with denoising diffusion GANs. In *International Conference on Learning Representations*, 2022. URL <https://openreview.net/forum?id=JprM0p-q0Co>.
- Zhengming Xing, Mingyuan Zhou, Alexey Castrodad, Guillermo Sapiro, and Lawrence Carin. Dictionary learning for noisy and incomplete hyperspectral images. *SIAM Journal on Imaging Sciences*, 5(1):33–56, 2012.
- Tao Xu, Pengchuan Zhang, Qiuyuan Huang, Han Zhang, Zhe Gan, Xiaolei Huang, and Xiaodong He. AttnGAN: Fine-grained text to image generation with attentional generative adversarial networks. In *CVPR*, pages 1316–1324, 2018.
- Xingqian Xu, Zhangyang Wang, Eric Zhang, Kai Wang, and Humphrey Shi. Versatile diffusion: Text, images and variations all in one diffusion model. *arXiv preprint arXiv:2211.08332*, 2022.
- Yanwu Xu, Yang Zhao, Zhisheng Xiao, and Tingbo Hou. UFOGen: You forward once large scale text-to-image generation via diffusion GANs. *ArXiv*, abs/2311.09257, 2023.
- Yue Yang, Ryan Martin, and Howard Bondell. Variational approximations using Fisher divergence. *arXiv preprint arXiv:1905.05284*, 2019.
- Mingzhang Yin and Mingyuan Zhou. Semi-implicit variational inference. In *International Conference on Machine Learning*, pages 5660–5669, 2018.
- Tianwei Yin, Michael Gharbi, Richard Zhang, Eli Shechtman, Frédo Durand, William T. Freeman, and Taesung Park. One-step diffusion with distribution matching distillation. *ArXiv*, abs/2311.18828, 2023.
- Jiahui Yu, Yuanzhong Xu, Jing Yu Koh, Thang Luong, Gunjan Baid, Zirui Wang, Vijay Vasudevan, Alexander Ku, Yinfei Yang, Burcu Karagol Ayan, et al. Scaling autoregressive models for content-rich text-to-image generation. *Transactions on Machine Learning Research*, 2022.
- Longlin Yu and Cheng Zhang. Semi-implicit variational inference via score matching. In *The Eleventh International Conference on Learning Representations*, 2023. URL <https://openreview.net/forum?id=sd90a2ytrt>.
- Longlin Yu, Tianyu Xie, Yu Zhu, Tong Yang, Xiangyu Zhang, and Cheng Zhang. Hierarchical semi-implicit variational inference with application to diffusion model acceleration. In *Thirty-seventh Conference on Neural Information Processing Systems*, 2023. URL <https://openreview.net/forum?id=ghIBaprxsV>.
- Han Zhang, Tao Xu, Hongsheng Li, Shaoting Zhang, Xiaogang Wang, Xiaolei Huang, and Dimitris N Metaxas. StackGAN: Text to photo-realistic image synthesis with stacked generative adversarial networks. In *Proceedings of the IEEE international conference on computer vision*, pages 5907–5915, 2017.
- Han Zhang, Weichong Yin, Yewei Fang, Lanxin Li, Boqiang Duan, Zhihua Wu, Yu Sun, Hao Tian, Hua Wu, and Haifeng Wang. ERNIE-ViLG: Unified generative pre-training for bidirectional vision-language generation. *arXiv preprint arXiv:2112.15283*, 2021.
- Hao Zhang, Bo Chen, Long Tian, Zhengjue Wang, and Mingyuan Zhou. Variational hetero-encoder randomized gans for joint image-text modeling. In *International Conference on Learning Representations*, 2020. URL <https://openreview.net/forum?id=H1x5wRVtvS>.
- Qinsheng Zhang and Yongxin Chen. Fast sampling of diffusion models with exponential integrator. In *The Eleventh International Conference on Learning Representations*, 2023. URL <https://openreview.net/forum?id=Loek7hfb46P>.

- Wenliang Zhao, Lujia Bai, Yongming Rao, Jie Zhou, and Jiwen Lu. Unipc: A unified predictor-corrector framework for fast sampling of diffusion models. *arXiv preprint arXiv:2302.04867*, 2023.
- Hongkai Zheng, Weili Nie, Arash Vahdat, Kamyar Azizzadenesheli, and Anima Anandkumar. Fast sampling of diffusion models via operator learning. In *International Conference on Machine Learning*, pages 42390–42402. PMLR, 2023a.
- Huangjie Zheng, Pengcheng He, Weizhu Chen, and Mingyuan Zhou. Truncated diffusion probabilistic models and diffusion-based adversarial auto-encoders. In *The Eleventh International Conference on Learning Representations*, 2023b. URL <https://openreview.net/forum?id=HDxgaKk9561>.
- Huangjie Zheng, Zhendong Wang, Jianbo Yuan, Guanghan Ning, Pengcheng He, Quanzeng You, Hongxia Yang, and Mingyuan Zhou. Learning stackable and skippable LEGO bricks for efficient, reconfigurable, and variable-resolution diffusion modeling. In *The Twelfth International Conference on Learning Representations*, 2024. URL <https://openreview.net/forum?id=qmXedvwrT1>.
- Mingyuan Zhou, Haojun Chen, John Paisley, Lu Ren, Guillermo Sapiro, and Lawrence Carin. Non-parametric Bayesian dictionary learning for sparse image representations. *Advances in neural information processing systems*, 22, 2009.
- Mingyuan Zhou, Tianqi Chen, Zhendong Wang, and Huangjie Zheng. Beta diffusion. In *Neural Information Processing Systems*, 2023. URL <https://arxiv.org/abs/2309.07867>.
- Mingyuan Zhou, Huangjie Zheng, Zhendong Wang, Mingzhang Yin, and Hai Huang. Score identity distillation: Exponentially fast distillation of pretrained diffusion models for one-step generation. In *Forty-first International Conference on Machine Learning*, 2024. URL <https://openreview.net/forum?id=QhqQJqe0Wq>.
- Yufan Zhou, Ruiyi Zhang, Changyou Chen, Chunyuan Li, Chris Tensmeyer, Tong Yu, Jiuxiang Gu, Jinhui Xu, and Tong Sun. Towards language-free training for text-to-image generation. In *Proceedings of the IEEE/CVF Conference on Computer Vision and Pattern Recognition*, pages 17907–17917, 2022.

Long and Short Guidance in Score identity Distillation for One-Step Text-to-Image Generation: Appendix

A Broader impact

The broader impact of our work is multifaceted. On one hand, it significantly reduces the energy required to operate state-of-the-art diffusion models, contributing to more sustainable AI practices. On the other hand, the ease of distilling and deploying models that might be trained on data with questionable content or intentions presents ethical challenges. Therefore, it is crucial for the community to engage in discussions on how to minimize risks while enhancing the benefits of such advancements. This involves developing robust guidelines and frameworks to govern the use and deployment of distilled models, ensuring they are used responsibly and ethically.

B Related work

Generative modeling of high-dimensional data has long been a focal point in machine learning research. This area primarily concentrates on replicating various data distributions: the original data distribution, conditional distributions influenced by labels, noisy or incomplete measurements, textual descriptions, or the joint distribution of data and other modalities. This has spurred the development of a diverse range of generative models and methodologies. Initially, these models were only capable of handling simpler, low-dimensional data such as 28×28 grayscale or binarized MNIST digits [Hinton et al., 2006, Salakhutdinov and Hinton, 2009, Vincent et al., 2010], vector-quantized local descriptors [Fei-Fei and Perona, 2005, Chong et al., 2009], or patches of natural and hyperspectral images [Zhou et al., 2009, Xing et al., 2012, Polatkan et al., 2015]. Early models often utilized neural networks with stochastic binary hidden layers or shallow hierarchical Bayesian models, which are simpler to train but have limited capacities.

Deep generative models. To tackle the generation of high-dimensional data, such as images comprising millions of pixels, substantial advancements in generative models have been made over the past decade. This period has marked the emergence of diverse deep generative models, including variational auto-encoders (VAEs) [Kingma and Welling, 2014, Rezende et al., 2014], normalizing flows [Papamakarios et al., 2019], generative adversarial networks (GANs) [Goodfellow et al., 2014, Reed et al., 2016, Karras et al., 2019, Wang et al., 2023b], autoregressive models [Gregor et al., 2015, Mansimov et al., 2015], and diffusion models [Sohl-Dickstein et al., 2015, Song and Ermon, 2019, Ho et al., 2020, Song and Ermon, 2020, Song et al., 2021b,a, Dhariwal and Nichol, 2021, Karras et al., 2022, Peebles and Xie, 2023, Zheng et al., 2024]. Additionally, essential resources for creating effective text-to-image synthesis systems, such as large language models [Vaswani et al., 2017, Devlin et al., 2018, Radford et al., 2018, 2019, Raffel et al., 2020, He et al., 2020, Brown et al., 2020, Achiam et al., 2023, Touvron et al., 2023, Jiang et al., 2023], large vision-language models [Radford et al., 2021, Ilharco et al., 2021, Cherti et al., 2023], advanced visual tokenization and compression [Rolfe, 2016, van den Oord et al., 2017, Esser et al., 2021, Rombach et al., 2022, Podell et al., 2024], and extensive training datasets [Thomee et al., 2016, Changpinyo et al., 2021, Schuhmann et al., 2022], have transitioned from proprietary tools of major tech companies to publicly available assets.

Previously, text-to-image models primarily utilized GANs and focused on small-scale, object-centric domains like flowers, birds, and face images [Reed et al., 2016, Zhang et al., 2017, Xu et al., 2018, Zhang et al., 2020]. Powered by text encoders that leverage pretrained large language models or vision-language models, which offer profound language comprehension and extract semantically rich latent representations, and supported by an extensive collection of text-image pairs, three main families of generative models—GANs [Zhou et al., 2022, Sauer et al., 2022, Kang et al., 2023], autoregressive models [Ramesh et al., 2021, Zhang et al., 2021, Ding et al., 2021, Gafni et al., 2022, Yu et al., 2022, Chang et al., 2023], and diffusion models [Nichol et al., 2022, Ramesh et al., 2022, Saharia et al., 2022, Rombach et al., 2022, Xu et al., 2022, Wang et al., 2023a, Qin et al., 2023]—have effectively capitalized on these technological advancements. These developments have facilitated the creation of text-to-image synthesis systems that demonstrate exceptional photorealism and sophisticated language understanding.

Acceleration of diffusion-based generation. Early-stage diffusion models were notably slow in sampling, spurring extensive research aimed at speeding up the reverse diffusion process. Researchers

have approached this by interpreting diffusion models through stochastic or ordinary differential equations and using advanced numerical solvers to enhance efficiency [Song et al., 2021c,a, Liu et al., 2022a, Lu et al., 2022b, Zhang and Chen, 2023, Karras et al., 2022]. Additional strategies include truncating the diffusion chain to initiate generation from more structured distributions [Pandey et al., 2022, Zheng et al., 2023b, Lyu et al., 2022], integrating these models with GANs to boost generation speed [Xiao et al., 2022, Wang et al., 2023b], and exploring flow matching in diffusion modeling [Liu et al., 2022b, Lipman et al., 2022, Albergo et al., 2023]. More recently, research has pivoted towards distilling reverse diffusion chains to refine and expedite the generation process, a direction that continues to evolve with new methodologies and insights [Luhman and Luhman, 2021, Salimans and Ho, 2022, Zheng et al., 2023a, Meng et al., 2023, Song et al., 2023, Song and Dhariwal, 2023, Kim et al., 2023, Sauer et al., 2023b, Xu et al., 2023, Yin et al., 2023, Luo et al., 2023c, Zhou et al., 2024].

Text-to-image diffusion distillation. Recent efforts aim to accelerate the sampling process from pre-trained diffusion teachers like SD [Rombach et al., 2022]. Sauer et al. [2023b] focused on distilling diffusion models into generators capable of one or two-step operations through adversarial training. Xu et al. [2023] introduced UFOGen, utilizing a time-step-dependent discriminator for generator initialization. Luo et al. [2023a] applied consistency distillation [Song et al., 2023] to text-guided latent diffusion models [Ramesh et al., 2022] for efficient, high-fidelity text-to-image generation. Building on the idea of using a pre-trained 2D text-to-image diffusion model for text-to-3D synthesis [Poole et al., 2022, Wang et al., 2023c], SwiftBrush [Nguyen and Tran, 2024] showcases its effectiveness of distilling pre-trained stable diffusion models. Distribution Matching Distillation (DMD) by Yin et al. [2023] further enhances distillation quality by adding a regression loss term.

C Training and evaluation details

The hyperparameters tailored for our study are outlined in Table 3. It’s important to note that the time and memory costs reported in Table 3 do not account for those incurred during periodic evaluations of the FID and CLIP scores of the single-step generator, nor do they include the resources used to save model checkpoints during the distillation process. These costs can vary significantly depending on the computing and storage platforms used and the frequency of these operations.

D Limitations and computational requirements

Memory and speed. Table 3 in Appendix C offers a detailed examination of the computational resources required for the SiD distillation process employing various CFG strategies—Long, Short, basic Long-Short, and the recommended Long-Short—across different NVIDIA GPU platforms (RTX-A5000 with 24GB, RTX-A6000 with 48GB, and H100 with 80GB). Key observations include:

SiD-LSG can be effectively run on the RTX-A5000 with 24GB memory by enabling xFormers [Lefaudeux et al., 2022] and switching to FP16 for model and gradient precision. On the RTX-A6000 with 48GB memory, it operates under FP32 with xFormers enabled. However, on our available H100 with 80GB memory, where xFormers are not supported, there is a noticeable increase in GPU memory consumption.

The recommended LSG strategy, which provides an improved balance between FID and CLIP scores, demands approximately 20% more computation time per iteration and exhibits about 10% more peak memory usage on the H100 compared to the Long or Short strategies. This underlines a trade-off between achieving performance enhancements and managing resource utilization.

FP16 versus FP32. SiD-LSG can be trained under FP16 mixed precision, which significantly conserves memory and enhances processing speed, as detailed in Table 3. Although this reduced precision in optimization leads to quicker improvements in both FID and CLIP scores, it also restricts the potential for achieving the lowest FID and highest CLIP scores compared to results under FP32. These effects are demonstrated in the ablation study shown in Figure 7. Additionally, FP16 operation is less stable and requires the use of gradient clipping to maintain training stability. For instance, we employ `torch.nn.utils.clip_grad_value_(G.parameters(), 1)` to prevent sudden model divergence—a precaution that is not necessary with FP32.

Table 3: Hyperparameter settings and comparison of distillation time and memory usage between different long and short guidance strategies of SiD. Note in order to run the long-short guidance (LSG) with $\kappa_1 = \kappa_2 = \kappa_3 = \kappa_4 > 1$, we need to turn off the EMA network for some cases (indicated with “no EMA”), otherwise it will be out of memory.

| Computing platform | Hyperparameters | Long Strategy | Short Strategy | Long-Short | Long-Short |
|-----------------------|----------------------------------|--------------------------------------|---|--|---|
| General Settings | CFG scales | $\kappa_4 > 1$ | $0 < \kappa_2 = \kappa_3 < 1$ | $\kappa_1 > 1$ | $\kappa_{1,2,3,4} > 1$ |
| | Batch size | $\kappa_1 = \kappa_2 = \kappa_3 = 1$ | $\kappa_1 = \kappa_4 = 1$ | $\kappa_2 = \kappa_3 = \kappa_4 = 1$ | $\kappa_1 = \kappa_2 = \kappa_3 = \kappa_4$ |
| | Learning rate | | | 512 | |
| | Half-life of EMA | | | 1e-6 | |
| | Optimizer under FP32 | | | 50k images | |
| | Optimizer under FP16 | | | Adam ($\beta_1 = 0, \beta_2 = 0.999, \epsilon = 1e-8$) | |
| | α | | | Adam ($\beta_1 = 0, \beta_2 = 0.999, \epsilon = 1e-6$) | |
| | Time parameters | | | 1.0 | |
| | | | $(t_{\min}, t_{\text{mit}}, t_{\max}) = (20, 625, 979)$ | | |
| RTX-A5000 (24G), FP16 | xFormers available and enabled | | | Yes | |
| | Batch size per GPU | | | 1 | |
| | # of GPUs | | | 8 | |
| | # of gradient accumulation round | | | 64 | |
| | Max memory in GB allocated | 22.9 | 22.9 | 22.6 | 22.0 (no EMA) |
| | Max memory in GB reserved | 23.0 | 23.0 | 23.0 | 22.1 (no EMA) |
| | Time in seconds per 1k images | 74 | 75 | 80 | 102 |
| | Time in hours per 1M images | 21 | 21 | 22 | 29 |
| RTX-A6000 (48G), FP32 | xFormers available and enabled | | | Yes | |
| | Batch size per GPU | | | 1 | |
| | # of GPUs | | | 8 | |
| | # of gradient accumulation round | | | 64 | |
| | Max memory in GB allocated | 45.7 | 45.7 | 45.0 | 45.8 (no EMA) |
| | Max memory in GB reserved | 45.7 | 45.7 | 45.9 | 46.0 (no EMA) |
| | Time in seconds per 1k images | 365 | 365 | 366 | 502 |
| | Time in hours per 1M images | 102 | 102 | 102 | 139 |
| H100 (80G), FP16 | xFormers available and enabled | | | No | |
| | Batch size per GPU | | | 4 | |
| | # of GPUs | | | 8 | |
| | # of gradient accumulation round | | | 16 | |
| | Max memory in GB allocated | 55.8 | 55.8 | 47.7 | 63.9 |
| | Max memory in GB reserved | 57.3 | 58.3 | 49.2 | 65.4 |
| | Time in seconds per 1k images | 17 | 17 | 18 | 23 |
| | Time in hours per 1M images | 5 | 5 | 5 | 6 |
| H100 (80G), FP32 | xFormers available and enabled | | | No | |
| | Batch size per GPU | | | 1 | |
| | # of GPUs | | | 8 | |
| | # of gradient accumulation round | | | 64 | |
| | Max memory in GB allocated | 58.9 | 57.4 | 53.4 | 62.9 |
| | Max memory in GB reserved | 60.0 | 59.0 | 54.0 | 64.0 |
| | Time in seconds per 1k images | 74 | 74 | 76 | 90 |
| | Time in hours per 1M images | 21 | 21 | 21 | 25 |

Further investigation is required to optimize FP16 performance to equal that of FP32, potentially through refined loss scaling techniques or by implementing an effective warmup period using FP16 before transitioning to FP32. We plan to address these challenges in future studies.

Reaching a performance plateau. Zhou et al. [2024] demonstrate through extensive comparisons that the SiD distilled one-step generator can reduce the FID at an exponential decay rate, showing a log-log linear relationship between the number of iterations and FID. This approach can match or even surpass the performance of both unconditional and label-conditional teacher diffusion models trained under the EDM framework [Karras et al., 2022], provided sufficient training.

However, results shown in Figures 4 and 5 indicate that the SiD-LSG distilled one-step generator on SD1.5 quickly reaches a performance plateau in reducing FID and/or increasing CLIP scores, particularly when the LSG scale exceeds 2. Additionally, data from Table 1 demonstrate that after processing 10M images (approximately 20k iterations at a batch size of 512), SiD-LSG still does not match the text-image alignment performance of the teacher model, which achieves higher CLIP scores after 250 generation steps. Notably, by reducing the LSG scale to 1.5 and doubling the training duration, SiD-LSG achieves a record-low FID of 8.15, establishing a new benchmark among all diffusion distillation methods. This achievement also surpasses the teacher model’s FID of 8.78, which was obtained with a CFG scale of 3 and 250 generation steps. However, this reduction in the LSG scale to 1.5 also results in a significant decline in its CLIP score.

This suggests significant potential for further performance enhancements, possibly by extending beyond single-step generation, increasing the model size, or incorporating real data and additional regression or adversarial losses into the distillation process. These avenues for improvement will be the focus of future studies.

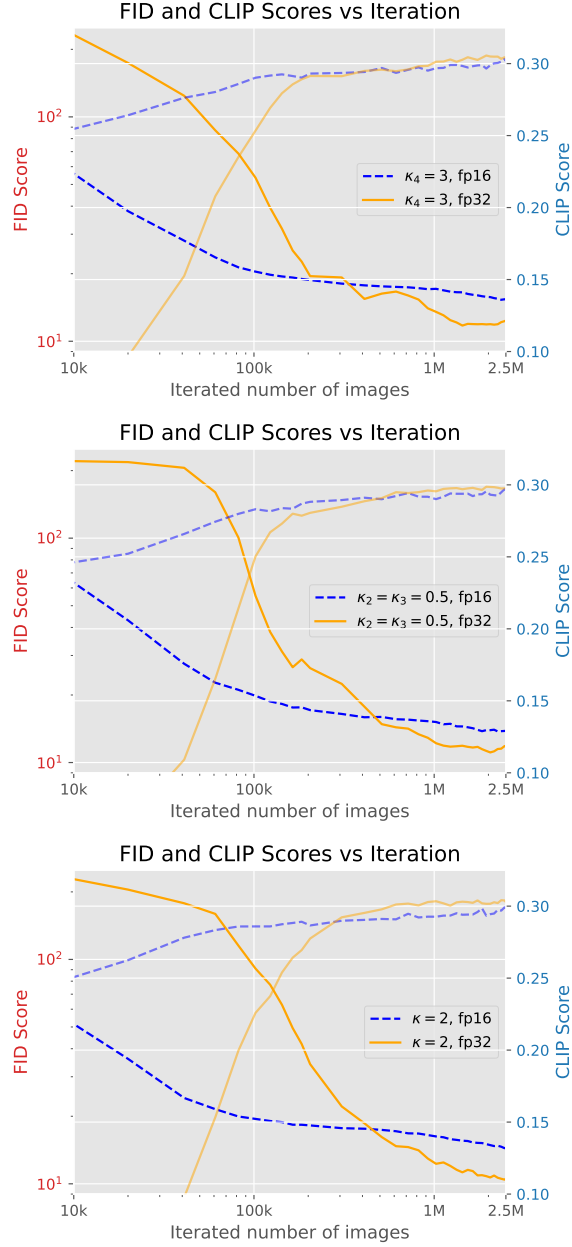


Figure 7: Comparison between FP16 and FP32 under three different guidance strategies. Top: Long strategy with $\kappa_1 = \kappa_2 = \kappa_3 = 1$ and $\kappa_4 = 3$. Middle: Short strategy with $\kappa_1 = \kappa_4 = 1$ and $\kappa_2 = \kappa_3 = 0.5$. Bottom: Long-short guidance (LSG) with $\kappa_1 = \kappa_2 = \kappa_3 = \kappa_4 = 2$.

E Prompts and additional example images

We list the prompts used in Figure 1 as follows:

1. A distinguished older gentleman in a vintage study, surrounded by books and dim lighting, his face marked by wisdom and time. 8K, hyper-realistic, cinematic, post-production.
2. saharian landscape at sunset , 4k ultra realism, BY Anton Gorlin, trending on artstation, sharp focus, studio photo, intricate details, highly detailed, by greg rutkowski.
3. chinese red blouse, in the style of dreamy and romantic compositions, floral explosions.
4. Digital 2D, Miyazaki's style, ultimate detailed, tiny finest details, futuristic, sci-fi, magical dreamy landscape scenery, small cute girl living alone with plushified friendly big tanuki in the gigantism of wilderness, intricate round futuristic simple multilayered architecture, habitation cabin in the trees, dramatic soft lightning, rule of thirds, cinematic.
5. poster art for the collection of the asian woman, in the style of gloomy, dark orange and white, dynamic anime, realistic watercolors, nintencore, weathercore, mysterious realism.
6. A fantasy-themed portrait of a female elf with golden hair and violet eyes, her attire shimmering with iridescent colors, set in an enchanted forest. 8K, best quality, fine details.
7. very beautiful girl in bright leggings, white short top, charismatic personality, professional photo, style of jessica drossin, super realistic photo, hyper detail, great attention to skin and eyes, professional photo.
8. (steampunk atmosphere, a stunning girl with a mecha musume aesthetic, adorned in intricate cyber gogle,) digital art, fractal, 32k UHD high resolution, highres, professional photography, intricate details, masterpiece, perfect anatomy, cinematic angle , cinematic lighting, (dynamic warrior pose:1)
9. (Pirate ship sailing into a bioluminescence sea with a galaxy in the sky), epic, 4k, ultra.
10. tshirt design, colourful, no background, yoda with sun glasses, dancing at a festival, ink splash, 8k.

We list the prompts used in Figure 2, which are taken from the COCO-2014 validation set, as follows:

1. many cars stuck in traffic on a high way
2. an old blue car with a surfboard on top', 3. 'a sole person sits in the front pew of a large church.
3. a shot of the hollywood sign at santa monica blvd.
4. a bunch of flowers, in front of a forest.
5. there is some sort of vegetables in a bowl
6. a man in a pink shirt stands staring against a green wall.
7. small girl in green shirt holding a slice of pizza to her face
8. two dogs sitting in the back seat of a car looking out the windwo

We list the prompts used in Figure 6 as follows:

1. Half-length head portrait of the goddess of autumn with wheat ears on her head, depicted as dreamy and beautiful, by wlop.
2. Walter White dressed as a medieval-style king.
3. A serene meadow with a tree, river, bridge, and mountains in the background under a slightly overcast sunrise sky.
4. A closeup portrait of a gray owl with spreaded wings attacking in cinematic lighting, digital painting by Greg Rutkowski used as album cover art on Artstation.
5. A hyena fursona sitting in the grass in a savannah at sunset.
6. A puppy staring through a red sectioned window.

We list the prompts used in Figure 8 as follows:

1. A fantasy-themed portrait of a female elf with golden hair and violet eyes, her attire shimmering with iridescent colors, set in an enchanted forest. 8K, best quality, fine details.
2. pumpkins, autumn sunset in the old village, cobblestone houses, streets, plants, flowers, entrance, realistic, stunningly beautiful.
3. Highly detailed mysterious egyptian (sphinx cat), skindentation:1.2, bright eyes, ancient egypt pyramid background, photorealistic, (hyper-realistic:1.2), cinematic, masterpiece:1.1, cinematic lighting.
4. vw bus, canvas art, abstract art printing, in the style of brian mashburn, light red and light brown, theo prins, charming character illustrations, pierre pellegrini, vintage cut-and-paste, rusty debris.
5. painterly style, seductive female League of legends Jinx character fighting at war, raging, crazy smile, crazy eyes, rocket lancer, guns, crazy face expression, character design, body is adorned with glowing golden runes, intense green aura around her, body dynamic epic action pose, intricate, highly detailed, epic and dynamic composition, dynamic angle, intricate details, multicolor explosion, blur effect, sharp focus, uhd, hdr, colorful shot, stormy weather, tons of flying debris around her, dark city background.
6. A charismatic chef in a bustling kitchen, his apron dusted with flour, smiling as he presents a beautifully prepared dish. 8K, hyper-realistic, cinematic, post-production.
7. A young adventurer with tousled hair and bright eyes, wearing a leather jacket and a backpack, ready to explore distant lands. 8K, hyper-realistic, cinematic, post-production.
8. A watercolor painting of a vibrant flower field in spring, with a rainbow of blossoms under a bright blue sky. 8K, best quality, fine details.
9. digital art of a beautiful tiger pokemon under an apple tree, cartoon style,Matte Painting,Magic Realism,Bright colors,hyper quality,high detail,high resolution.
10. painterly style, Goku fighting at war, raging, blue hair, character design, body is adorned with glowing golden runes, yellow aura around him, body dynamic epic action pose, intricate, highly detailed, epic and dynamic composition, dynamic angle, intricate details, multicolor explosion, blur effect, sharp focus, uhd, hdr, colorful shot, stormy weather, tons of flying debris around him, dark city background.
11. A stunning steampunk city with towering skyscrapers and intricate clockwork mechanisms, gears and pistons move in a complex symphony, steam billows from chimneys, airships navigate the bustling skylanes, a vibrant metropolis.
12. Samurai looks at the enemy, stands after the battle, fear and horror on his face, tired and beaten, sand on his face mixed with sweat, an atmosphere of darkness and horror, hyper realistic photo, In post - production, enhance the details, sharpness, and contrast to achieve the hyper - realistic effect.
13. A portrait of an elemental entity with strong rim lighting and intricate details, painted digitally by Alvaro Castagnet, Peter Mohrbacher, and Dan Mumford.
14. A regal female portrait with an ornate headdress decorated with colorful gemstones and feathers, her robes rich with intricate designs and bright hues. 8K, best quality, fine details.
15. A detailed painting of Atlantis by multiple artists, featuring intricate detailing and vibrant colors.
16. A landscape featuring mountains, a valley, sunset light, wildlife and a gorilla, reminiscent of Bob Ross's artwork.

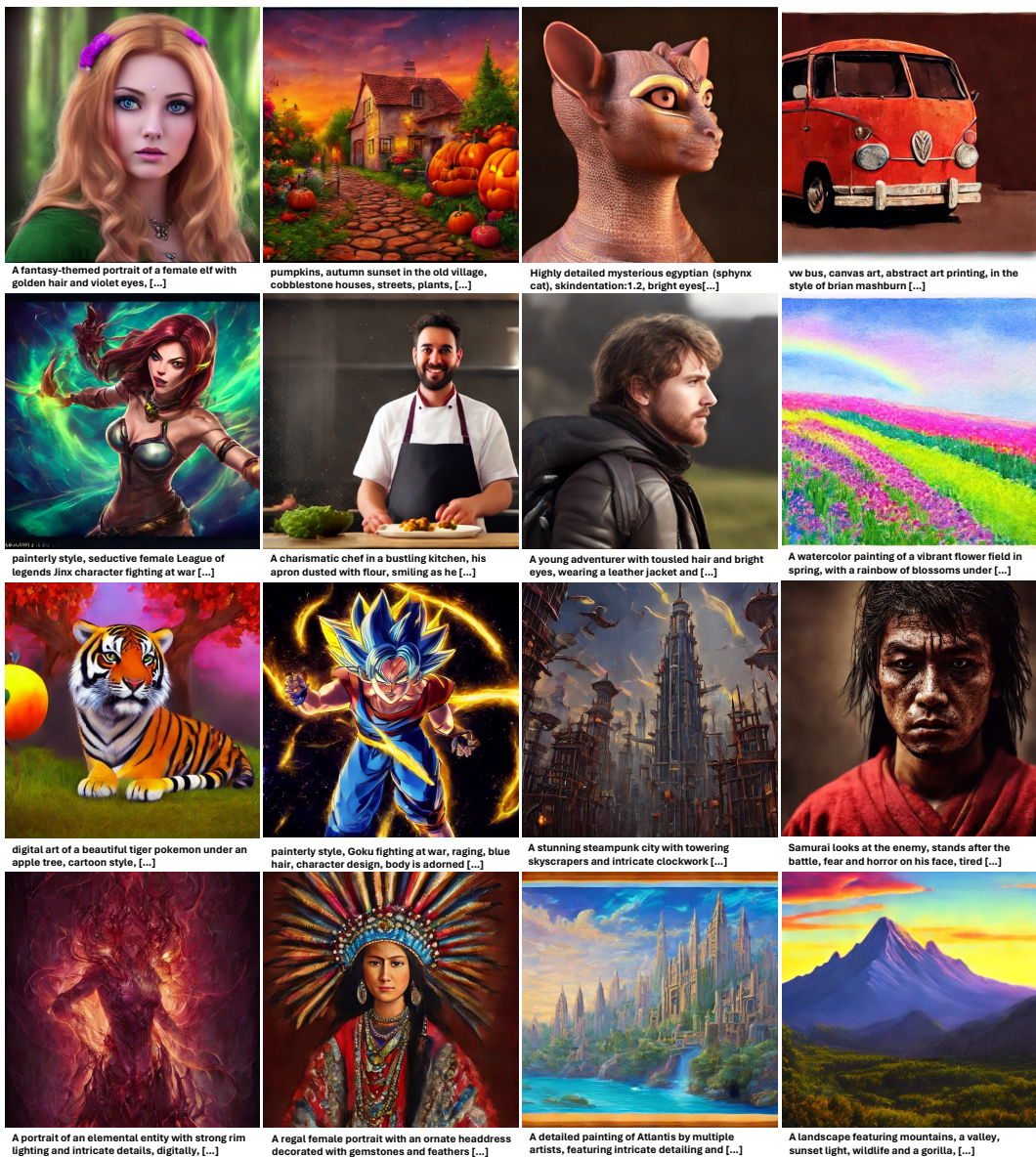


Figure 8: More examples from the one-step generator distilled from Stable Diffusion 2.1-base using the proposed method: Score identity Distillation with Long-Short Guidance.